



Technical Memorandum 47

# Techniques for the analysis of radionuclides in the environment and their application — Part 1

Riaz Akber and Paul Martin

Supervising Scientist for  
the Alligator Rivers Region

Supervising Scientist for the  
Alligator Rivers Region

**Technical memorandum 47**

**Techniques for the analysis of  
radionuclides in the environment  
and their application  
Part 1**

Edited by Riaz Akber and Paul Martin



Australian Government Publishing Service  
Canberra 1994

This Technical memorandum was edited by

Riaz Akber and Paul Martin

with contributions by Riaz Akber, Gary Hancock, Rainer Marten, Paul Martin,  
John Pfitzner and Stewart Whittlestone

Stewart Whittlestone – Australian Nuclear Science and Technology  
Organisation, PMB 1, Menai NSW 2234 Australia

---

© Commonwealth of Australia 1994

Supervising Scientist for the Alligator Rivers Region  
GPO Box 407, Canberra ACT 2601 Australia

**ISSN 0810 9532**

This work is copyright. Apart from any use as permitted under the Copyright Act 1968, no part may be reproduced by any process without prior written permission from the Australian Government Publishing Service. Requests and inquiries concerning reproduction and rights should be addressed to the Manager, Commonwealth Information Services, Australian Government Publishing Service, GPO Box 84, ACT 2601.

Views expressed by authors do not necessarily reflect the views and policies of the Supervising Scientist, the Commonwealth Government or any collaborating organisation.

Printed for AGPS by NTUniprint

---

# Contents

<b>Preface</b>	v
----------------	---

## **Paper 1**

*R Marten*

Quality assurance for low level gamma spectroscopy using HPGe-detectors	1
---	---

## **Paper 2**

*RA Akber, J Pfitzner & S Whittlestone*

A mobile station for radon measurements	11
---	----

## **Paper 3**

*G Hancock, P Martin & RA Akber*

Determination of $^{227}\text{Ac}$ by alpha-particle spectrometry	23
---	----

## **Paper 4**

*G Hancock & P Martin*

A method for the determination of all radium isotopes in groundwaters by alpha-particle spectrometry	29
--	----

## **Paper 5**

*P Martin & RA Akber*

Radium isotopes as seepage indicators in the vicinity of a uranium tailings dam	39
---	----

## **Figures**

### **Paper 1**

1 Bias and precision (from W Hendee 1984)	3
2 Interlaboratory comparison exercise IAEA/SL-2, results for $^{226}\text{Ra}$ (from LaBrecque et al 1987). Systematic bias between the participating laboratories is clearly visible.	3
3 Stability of the efficiency of a detector using a standard source containing $^{238}\text{U}$ and $^{232}\text{Th}$ . Deviations show at 'M' a misplacement of the sample and at 'A' reduced efficiency over a period of uncontrolled conditions.	4
4 Background stability for a detector showing stable conditions after being placed in final shield configuration	6
5 History of background checks showing effects of replacement of the detector entrance window (E). The original beryllium was substituted by selected magnesium. (R) indicates a repair period.	7
6 Background of a detector with internal thorium contamination	8
7 Effect of cryostat vacuum on energy resolution	9

## Paper 2

1	A locality map	13
2	A block diagram of the mobile radon station equipment	14
3	Diurnal variations in average monthly radon concentrations	15
4	Average monthly radon daughter concentrations as a function of the time of the day. The relative radon concentrations (dotted lines) are also shown for comparing the trends. The equilibrium factors (dashed lines) are calculated using half-hourly radon and radon daughter concentration data.	17
5	The wind direction distribution in Jabiru East during the months of January and June, 1990. The left hand side of the figure shows the variations in the average wind speeds as the time of the day.	18
6	Radon concentrations vs. wind speed for the January 1990 and June 1990 (overlay)	20
7	Radon concentrations in different wind sectors in Jabiru East (a) January 1990 and (b) June 1990	20

## Paper 3

1	a An actinium source counted immediately after electrodeposition	26
	b The same source counted three months later	26
2	The $^{235}\text{U}$ decay series	27
3	$^{227}\text{Th} + ^{223}\text{Ra}$ ingrowth and $^{225}\text{Ac}$ decay from an initially pure actinium source	27

## Paper 4

1	Flow diagram for the radiochemical separation of radium	31
2	a A typical groundwater sample counted immediately after deposition. 78 ksec count, FWHM of the $^{226}\text{Ra}$ peak is 38 keV.	32
	b The same disc counted 20 days after deposition.	32
	c The same disc counted 6 months after deposition.	32

## Paper 5

1	Location of the Ranger uranium mine	40
2	Ranger bore location plan	40
3	Cation and anion ternary diagrams for boreholes in the vicinity of the Ranger tailings dam	42
4	Bore OB11A $^{226}\text{Ra}$ and sulphate concentrations	42
5	$^{223}\text{Ra}/^{226}\text{Ra}$ vs. sulphate for a number of bores near the Ranger tailings dam	46

---

## Preface

The Alligator Rivers Region Research Institute (ARRRI)<sup>1</sup> undertakes research into the effects on the environment of uranium mining operations in the Alligator Rivers Region of the Northern Territory. The Environmental Radioactivity section of ARRRI carries out research related to the protection of humans from radiological hazard. This work has required the development of a number of techniques for radionuclide measurement and their application to studies of the transport of radionuclides through the environment.

In April 1985 a workshop entitled 'Measurement of Long-lived Environmental Radionuclides' was held in Sydney, New South Wales. Four papers were presented by officers of ARRRI, covering the topics of gamma spectrometry, alpha spectrometry and gross alpha counting, and were published in the workshop proceedings. In September 1990 a second workshop, entitled 'Environmental Radiochemistry and Radionuclide Measurement', was held in Adelaide, South Australia. As an outgrowth of these workshops, a formal association of scientists involved in environmental radioactivity studies in the South Pacific region has been formed. Called the South Pacific Environmental Radioactivity Association (SPERA), this organisation has now held workshops in Tahiti (1991), Dunedin (1992) and Canberra (1994), with the next meeting scheduled for Darwin in 1996.

Five papers presented by staff of ARRRI at the 1990 workshop in Adelaide have been prepared in written form. They are being presented here as a Technical memorandum in the Supervising Scientist's publication series to ensure that the information contained in them is given more widespread distribution.

RIAZ AKBER  
PAUL MARTIN

---

<sup>1</sup> Since the papers in this publication were presented, ARRRI has merged with the Commonwealth's Environment Protection Agency, and is now called the Environmental Research Institute of the Supervising Scientist (ERISS). However, the name ARRRI will continue to be used in this publication.

## Quality assurance for low level gamma spectroscopy using HPGe-detectors

R Marten

---

### Abstract

This presentation is based on six years experience with seven HPGe-detector systems (ie high purity germanium, coaxial, n-type or p-type). Routine stability checks of background and efficiency are described. Interlaboratory comparisons are discussed as an essential exercise to confirm the accuracy of results. Examples demonstrate typical problems and the importance of routine quality control procedures. An example of maintenance of a HPGe-detector is also included.

---

### Introduction

High purity germanium detectors are commonly used for low level gamma-ray spectroscopy. Topics essential for this application are covered in comprehensive books, such as Knoll (1979) and Debertin & Helmer (1988). This paper reports on the aspect of quality assurance and methods used in this laboratory. The objective of quality assurance is to ensure, with a high degree of confidence, that results are accurate and experimental errors are reliable.

The degree of quality of the analysis of radionuclides is represented in fig 1, displaying the influence of different sources of errors on a series of individual measurements. It shows that in order to achieve an unbiased and precise result, the sum of systematic and random errors must be small.

When all correcting measures have been applied to minimise faults, the result should be precise, ie a high degree of reproducibility of individual measurements is achieved. However, the possibility of a systematic bias remains and has to be investigated by intercomparison with other, preferably independent, analytical techniques, or by analysis of reference materials. Only then it can be assumed with a high degree of confidence that the results produced are both precise and accurate.

The significance of quality assurance can be demonstrated by examination of an interlaboratory comparison exercise conducted by the IAEA, Vienna. Twenty-one participating laboratories in fifteen countries returned results for the determination of environmental concentrations of radioactivity in a lake sediment (IAEA/SL-2).

Laboratories were requested to determine the following radionuclides:  $^{40}\text{K}$ ,  $^{90}\text{Sr}$ ,  $^{137}\text{Cs}$ ,  $^{226}\text{Ra}$ , and  $^{239/240}\text{Pu}$ . Data on other radionuclides were also welcomed. Sufficient data for consideration of assignment of recommended values were obtained for only three isotopes,

$^{137}\text{Cs}$ ,  $^{40}\text{K}$  and  $^{226}\text{Ra}$ . Even of these results,  $^{226}\text{Ra}$  did not meet the criteria for certification with only six results inside the 95% confidence interval (fig 2). The final report certifies  $^{40}\text{K}$  (245Bq/kg) and  $^{137}\text{Cs}$  (2.41Bq/kg) (LaBrecque et al 1987).

---

## Quality assurance at ARRI

The overall stability of HPGe-detector systems, including signal processing electronics, has improved considerably in recent years. Although this progress implies that regular performance checks are no longer necessary, experience shows that such checks should be implemented to ensure accuracy. At ARRI routine checks have been performed on a regular basis since 1983 (ARRI 1987). Examination of the system stability is inevitable after events such as detector warm-up, repairs, change of the amplifier time constant, change of the detector environment, or power failures. Routine checks include:

- stability of the detector efficiency
- stability of the detector background
- interlaboratory comparison exercises

Results of these checks are examined for trends and deviations outside the expected random variations. Instabilities of this nature can be caused by detector contamination, slight displacement of samples on the detector, electronics malfunctions, incorrect live-time, or detector warm-up.

### Stability of the detector efficiency

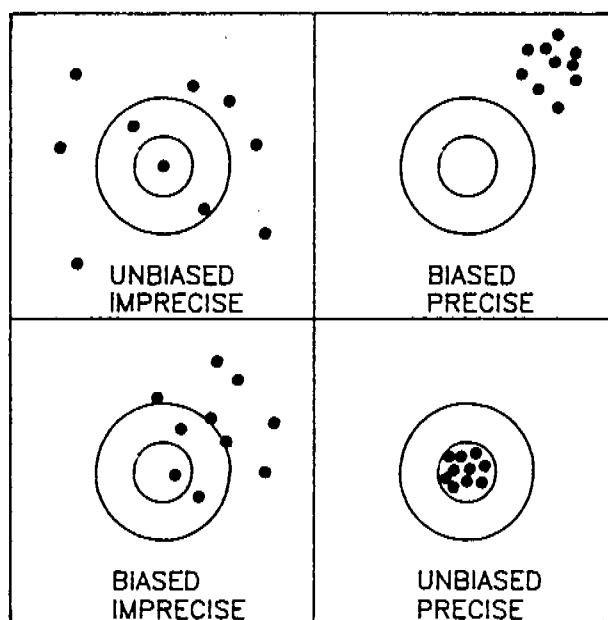
The stability of the detector efficiency is checked by counting a standard sample containing approximately equal activities of  $^{238}\text{U}$  and  $^{232}\text{Th}$  and their daughters in equilibrium. This spectrum is then analysed by using the routinely applied software (Murray et al 1987). The comparison of the results for each nuclide in the two decay series with previous results detects deviations from the expected means and enables timely action for recovery. A check of the detector resolution is also included, which may be performed on selected peaks of the spectrum. This simple and effective procedure is conducted at intervals of two weeks for each detector.

Figure 3 shows results of efficiency checks for a standard p-type detector for a period of five years. The results for  $^{238}\text{U}$  show a 'dip' for a period of time with a maximum decrease of 17%. This arose from an unusual gain shift, which was too large to be automatically compensated for by the analysis software. The gain change remained undetected because throughout this period the detector was operated by another group, and not examined according to standard procedure. The effect of this shift is especially high for  $^{238}\text{U}$ , because of the location in the spectrum of the low energy lines of  $^{234}\text{Th}$ , used to determine  $^{238}\text{U}$ . This problem ought to have been avoided by regular examination of the spectrum and consequent readjustment to the calibrated peak positions. However, the documentation of date, duration and magnitude of any effect allows for correction of results for samples which were analysed during this period.

### Stability of the detector background

A typical detector background is composed of an internal and external component. If there is no change in location, shielding materials and geometry, the background should be stable, although radon fluctuations in air can still produce a varying contribution. Another uncertain component of the total background is contamination—a particular risk when analysing liquid samples. The stability of the detector background is checked every four to six weeks by counting a blank sample for two to three days.





**Figure 1** Bias and precision (from W Hendee 1984)

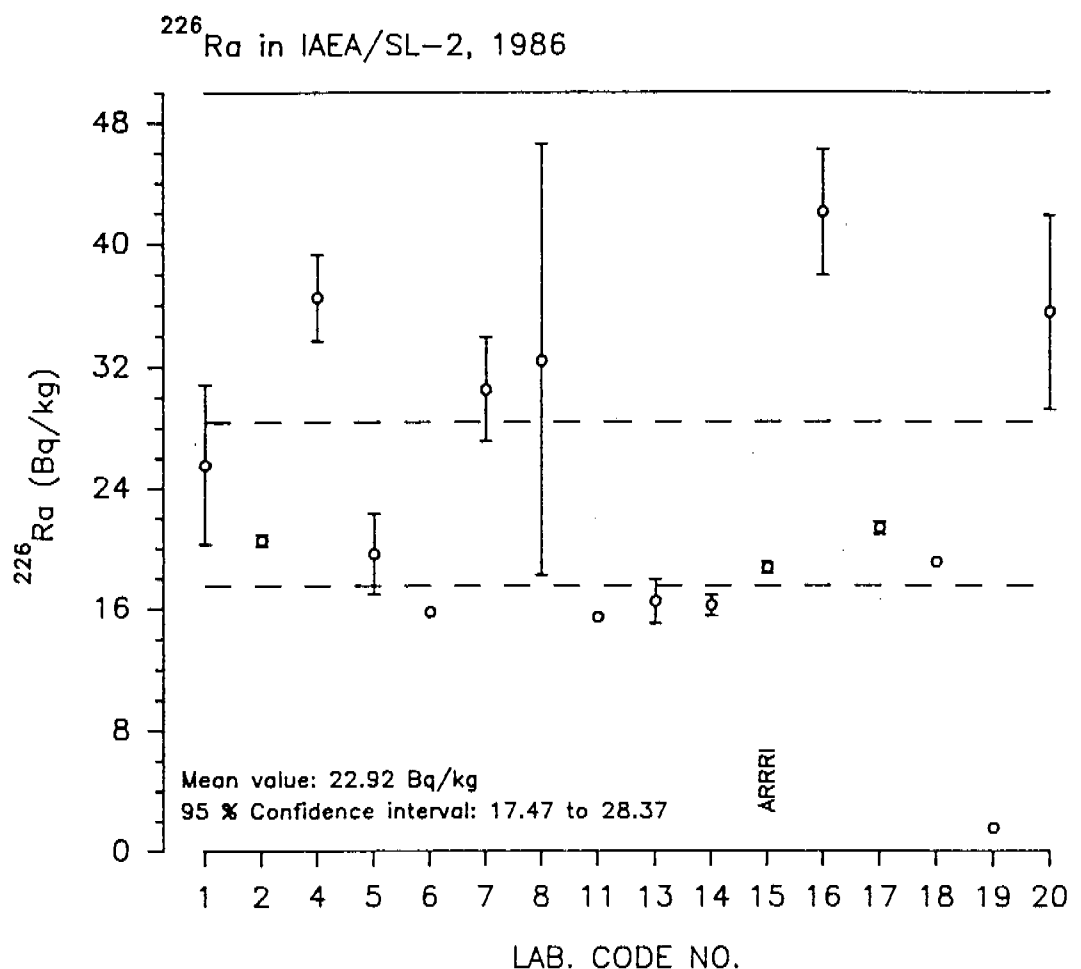


**Figure 2** Interlaboratory comparison exercise IAEA/SL-2, results for  $^{226}\text{Ra}$  (from LaBrecque et al 1987). Systematic bias between the participating laboratories is clearly visible.

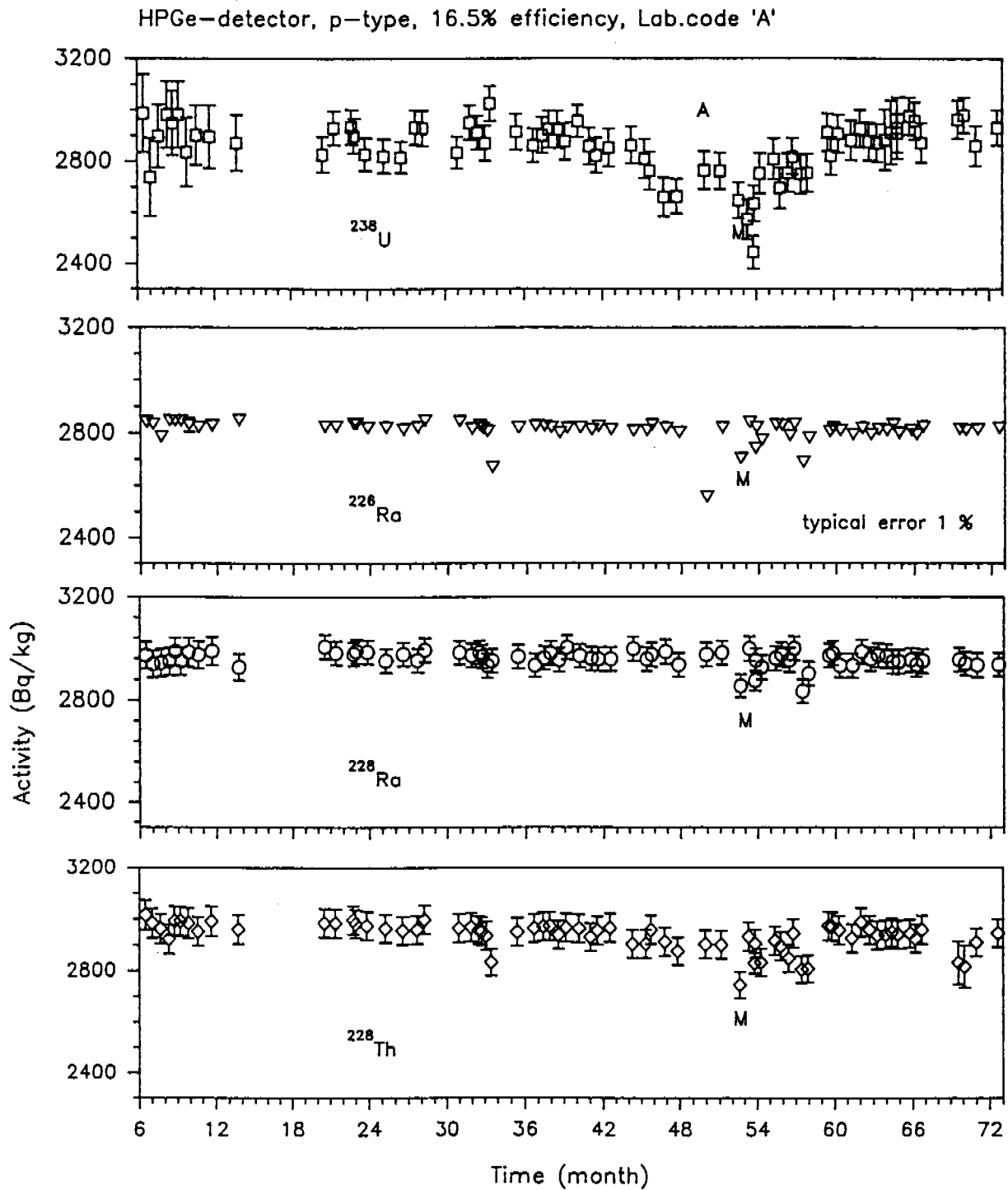


**Figure 3** Stability of the efficiency of a detector using a standard source containing  $^{238}\text{U}$  and  $^{232}\text{Th}$ . Deviations show at 'M' a misplacement of the sample and at 'A' reduced efficiency over a period of uncontrolled conditions.

Figure 4 shows typical results for stability checks of the background of an n-type, short coaxial detector over a period of 18 months. The graph illustrates that after installation and an experimental phase, the expected stability was achieved. The very low count rates for this detector are remarkable.

The effect of a change in the internal background of another detector is shown in fig 5. After an operating period of twenty months, the original beryllium window broke and was replaced by a window made of magnesium. The background of the 63 keV and 186 keV lines improved considerably due to the selected material and revealed the uranium impurities in the beryllium. Before and after this repair, no significant trends in the background were apparent. This graph also displays the effect of varying radon concentrations in the detector environment, leading to count rate fluctuations of the radon daughter lines.

An unusual example of a continuous background change is displayed in fig 6. Over the full period of six years the count rates from background peaks of  $^{232}\text{Th}$  daughter nuclides on this detector have risen steadily. It is apparent that this effect results from ingrowth of  $^{228}\text{Ra}$  from elemental thorium contamination of the construction materials used around the crystal. This example particularly demonstrates the importance of regular background checks to use the correct average value for the analysis of nuclide concentrations.

### Interlaboratory comparison exercises

Interlaboratory comparison exercises are conducted regularly by the Analytical Control Services of the IAEA, Vienna, using a wide variety of materials. For a meaningful participation, the selected sample material should be similar in composition and concentration to the samples analysed on a routine basis. In this application samples are analysed for naturally occurring radionuclides at environmental concentrations and the artificial radio isotope  $^{137}\text{Cs}$ . ARRRI has participated in IAEA intercomparison exercises on:

- lake sediment SL-2, 1986,
- marine fish flesh MA-B-3, 1986 and
- tuna fish flesh #352, 1989.

Table 1 shows results for  $^{137}\text{Cs}$  and  $^{40}\text{K}$  for these three intercomparison exercises.

**Table 1** Results of participation in IAEA interlaboratory exercises. Samples analysed were lake sediment (SL-2), marine fish flesh (MA-B-3), and tuna fish flesh (#352).

		IAEA	ARRRI
$^{137}\text{Cs}$	SL-2	2.4 (2.2–2.6)	$2.4 \pm 0.1$
	MA-B-3	14.2 (13.7–15.3)	$15.5 \pm 0.4$
	#352	2.7 (2.5–2.8)	$2.5 \pm 0.3$
$^{40}\text{K}$	SL-2	240 (211–269)	$237 \pm 6$
	MA-B-3	272 (252–299)	$272 \pm 6$
	#352	391 (379–405)	$379 \pm 16$

All results are in (Bq/kg) dry weight;

IAEA results are 'recommended mean value' with the 95% confidence interval;

ARRRI results are 'mean value  $\pm$  one standard deviation'.

The outcome of these exercises is often surprising and unexpected in terms of number of outliers, acceptable errors and the total number of nuclides certified. Intercomparison sample IAEA SL-2 has been discussed above as an example for the need of quality control to ensure accurate results.

HPGe-detector, n-type, short coaxial, Lab.code 'K'

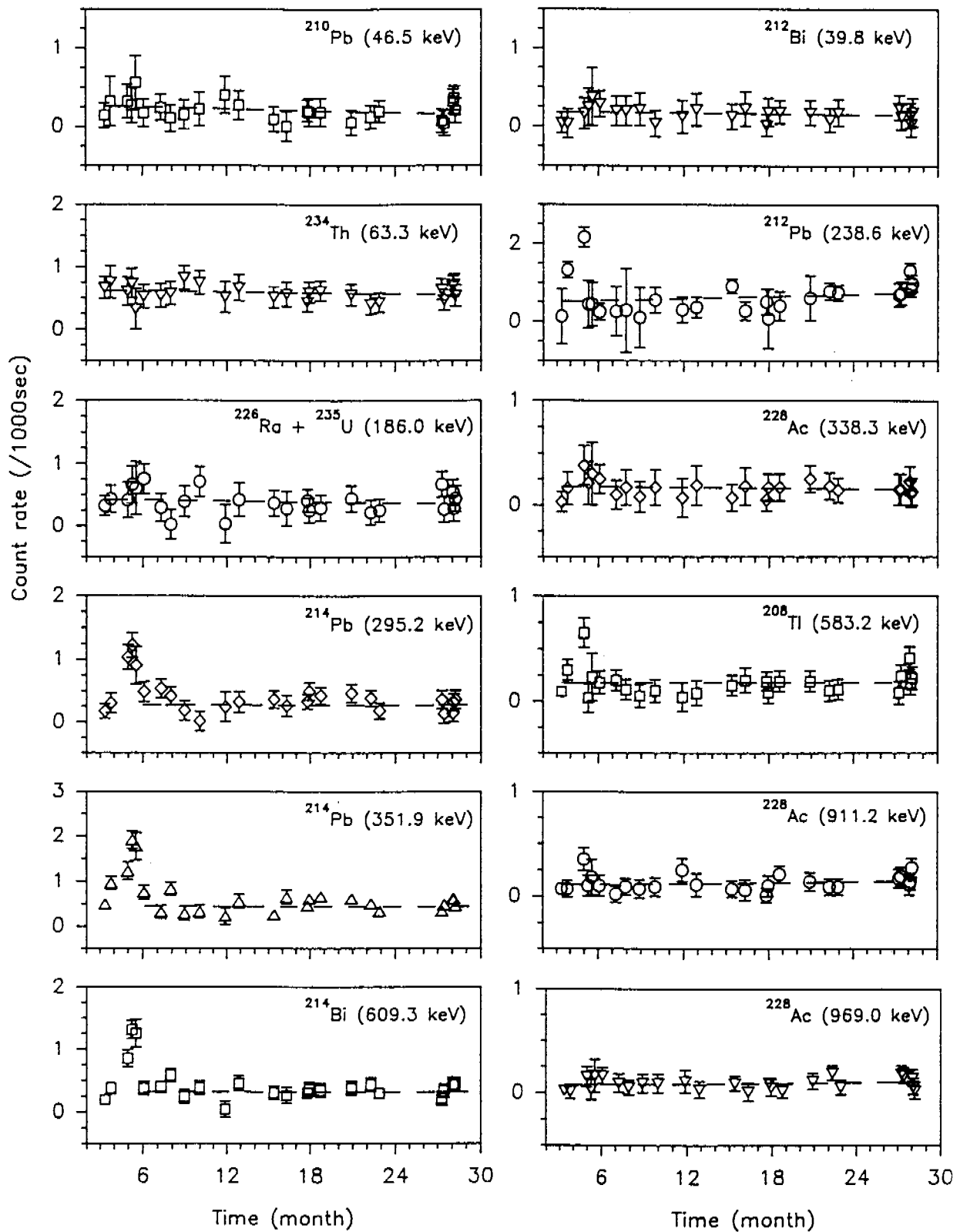
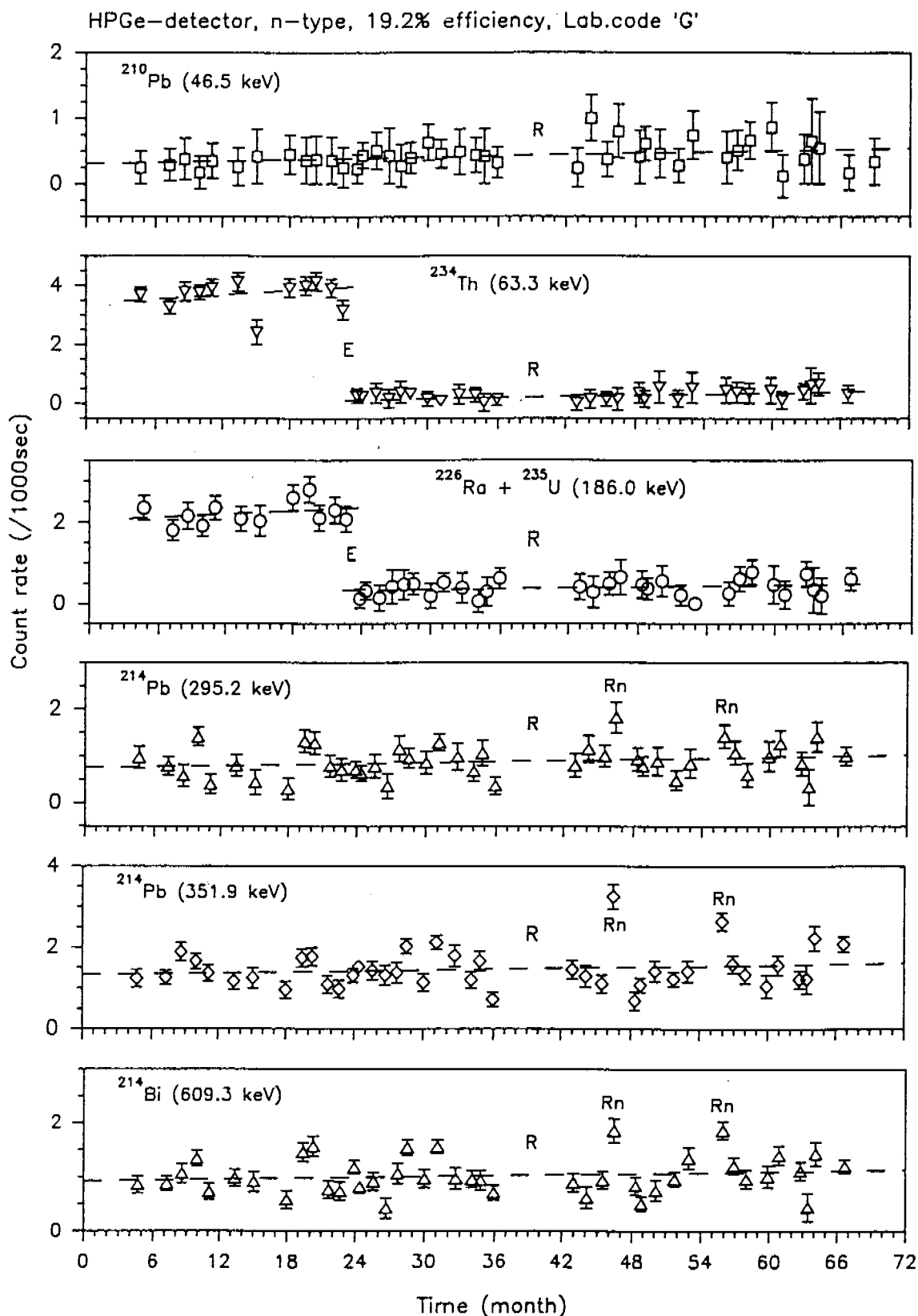


Figure 4 Background stability for a detector showing stable conditions after being placed in final shield configuration



**Figure 5** History of background checks showing effects of replacement of the detector entrance window (E). The original beryllium was substituted by selected magnesium. (R) indicates a repair period.

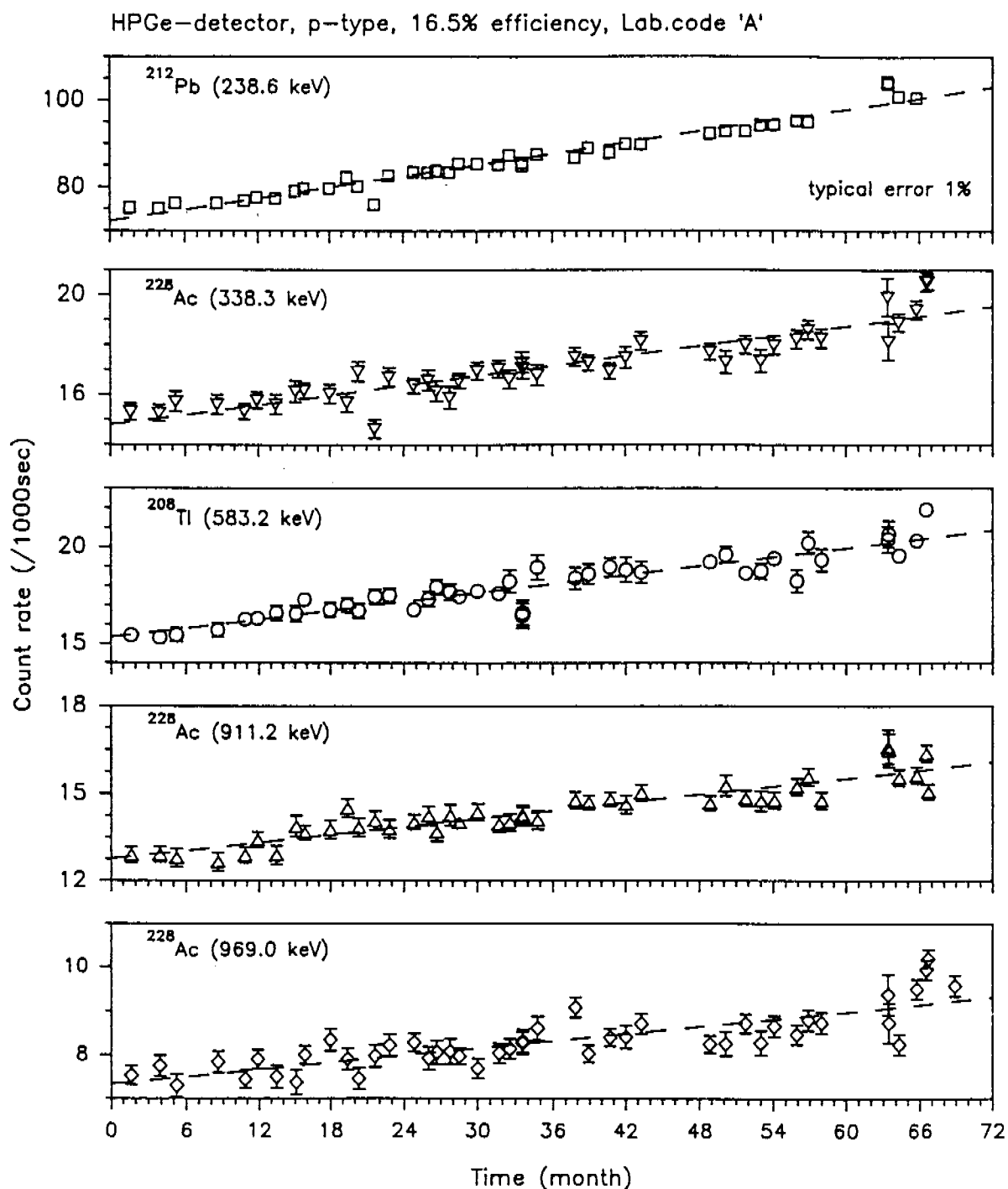


Figure 6 Background of a detector with internal thorium contamination

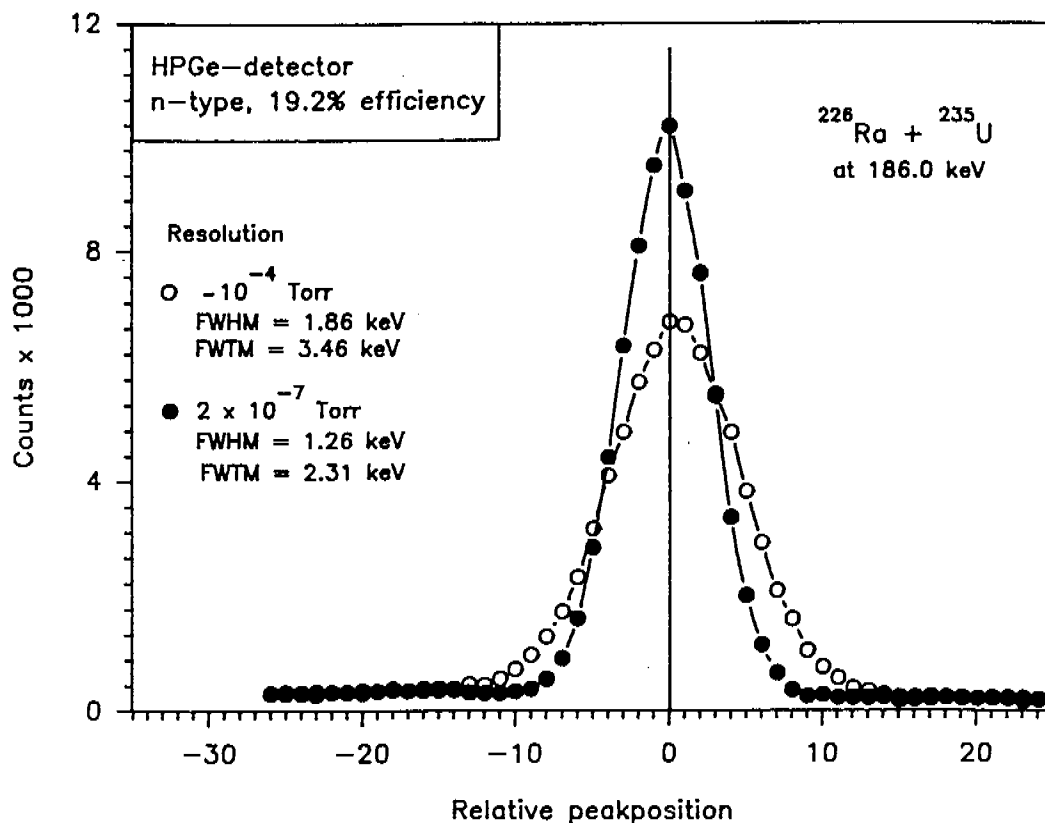


Figure 7 Effect of cryostat vacuum on energy resolution

An interlaboratory comparison exercise arranged nation-wide would be of significant benefit in order to ensure that all laboratories working in this field in Australia are able to produce the required precise and accurate results. The outcome could only improve quality standards.

### Effect of poor cryostat vacuum

One of the best indicators for the loss of performance of a HPGe-detector is a decreasing energy resolution and the associated peak-to-compton ratio. This particularly affects the analysis of complex spectra and samples with low activities.

The energy resolution of this type of detector is a combination of the effects of carrier statistics, charge carrier collection, leakage current, electronics noise, and instability of the electronics. An increase in leakage current or electronics noise can be observed as an increase of the FWHM (full width at half maximum) of a selected peak and the associated leakage current at the test point of the preamplifier. Both are specified by the detector manufacturer.

The leakage current is directly affected by the quality of the vacuum in the cryostat surrounding the germanium crystal. Figure 7 illustrates the effect of the cryostat vacuum. The detector resolution improved from FWHM = 1.86 keV to FWHM = 1.26 keV at 186 keV after evacuating the cryostat from approximately  $10^{-4}$  to better than  $2 \times 10^{-7}$  torr. In fact, the recovery was better than 30% for all peaks of the energy spectrum.

The main part of the pumping system used for this procedure at ARRRI is a 'turbomolecular pump'. This pump not only ensures the high vacuum required, but also generates an exceptionally clean vacuum, avoiding any possible surface contamination with oil vapour.

## **Conclusion**

Quality assurance for low level gamma spectroscopy using HPGe-detectors is a necessity in order to ensure precise and accurate analytical results. The procedures used at ARRRI are applied routinely and allow correction of analytical results even after a period of operation under inconsistent conditions. Furthermore, these procedures are simple, and supply the analyst with valuable knowledge of the condition of individual detectors, and a high degree of confidence in the results obtained.

---

## **Acknowledgment**

The author wishes to thank AS Murray for his contributions in establishing these quality assurance procedures at ARRRI.



## A mobile station for radon measurements

RA Akber, J Pfitzner and S Whittlestone<sup>1</sup>

---

### Abstract

An automatic radon monitoring station installed in a caravan has been operational since July 1989. The primary objective of the operation is to estimate the contribution of Ranger Uranium Mine to the atmospheric radon and radon daughter concentrations at selected locations within a few kilometres from the mine site. This has been achieved through simultaneous measurements of radon/radon daughter concentrations and meteorological variables, particularly wind direction. The basic operational principles of the equipment are described here with some illustrative examples.

---

### Introduction

Atmospheric transport of radon from a uranium mine is a potential pathway for radiation exposure of members of the public living in the vicinity of the mine site. The radon plume is likely to disperse with distance, hence the radiation exposure is expected to decrease with increasing distance between the mine site and a sampling point. Moreover, mine-related radon exposure may not be the same at two sampling points at the same distance but in different directions from the mine. This is because the wind may not blow with equal frequency in both directions.

Hence in order to make reliable estimates of radon transport, several measurements of both radon concentration and wind direction may be required at several sampling points relative to the mine. Results from one such study were reported by Whittlestone (1992). This study was conducted at the Ranger Uranium Mine in the Northern Territory of Australia. Five sampling stations were established, three at strategic locations within the mine site to estimate the relative significance of various potential sources, and one each in the nearby townships of Jabiru East and Jabiru, to measure the environmental concentrations of radon. However, it was realised that a mobile station may be a useful and manageable alternative to several stations maintained at different locations. A mobile station could operate at different locations for suitable intervals of time. The major limitation, however, would be the lack of data for simultaneous measurements at more than one sampling point.

In March 1989, we installed an automatic radon monitoring station in a caravan which became fully operational in July, 1989. Since then, and in conjunction with another similar fixed monitoring station, it has been used continuously for a research project to provide

---

<sup>1</sup> Stewart Whittlestone – Australian Nuclear Science and Technology Organisation, PMB 1, Menai NSW 2234 Australia

estimates of public radiation dose due to the operation of the Ranger Uranium Mine. Details of the public radiation dose are given by Akber et al (1991).

The objective of the present paper is mainly to describe the operational details of the equipment and some illustrative examples from the results. The illustrative examples used here are for the time periods when the mobile station was located either in Jabiru East or in Jabiru. Figure 1 shows the locality of these towns relative to the Ranger Uranium Mine.

---

## Rationale

The Australian code of practice for mining and milling of the radioactive ores requires that the operations are managed in such a way that members of the public do not receive a radiation dose above an internationally accepted limit of  $1 \text{ mSv y}^{-1}$  (Code 1987). All pathways of radiation exposure and the contribution of all different radionuclides need to be considered. Atmospheric concentrations of radon and radon daughters in the townships and Aboriginal camp sites a few kilometres from the Ranger Uranium Mine are expected to be due both to natural background sources and anthropogenic sources associated with the mining activities. A radon and radon daughter monitoring facility to make estimates of the radiation dose due to the mining operation should therefore, be able to distinguish between the contribution of these two types of sources. The monitoring equipment in the mobile radon station has been designed to make this distinction on the basis of correlated wind direction measurements (Akber et al 1991, Whittlestone 1992).

---

## Equipment

The method of correlated measurements of radon and radon daughter concentrations with the wind direction is a straight forward one. The signals in the wind sectors including the mine are distinguished from those including only the natural background sources. The difference between the two signals is then attributed to the sources associated with the mine. Experimentally, it requires simultaneous measurements of wind direction and atmospheric concentrations of radon and radon daughters.

Figure 2 is a block diagram of the station. Wind direction is averaged on a half-hourly basis and radon and radon daughter concentrations are measured for the same time period. Wind speed sensors are also incorporated into the system. The standard deviation of wind direction is calculated using a single pass filter method described in Yamartino (1984). Measurements of the unattached radon daughter concentrations and aerosol density of the ambient air are a developmental part of the project. They are not discussed in this report.

Meteorological measurements have been routinely carried out at the height of 12 m above the ground, away from the interference of arboreal canopy. Radon and radon daughter concentrations are measured either at the same height or at a height of 2 m or lower on a separate support.

The equipment is computer controlled and requires minimum operator intervention. All measurements are automatically recorded on floppy diskettes as a half-hourly time series. The data are later sorted for different correlations.

Power supply irregularities are reduced by the use of line filters and an uninterruptable power supply which can power the equipment for more than two hours in the event of mains failure. Further protection is provided by the use of optical fibre coupling between devices outside the caravan and the data acquisition system. A trailer mounted 5kVA generator allows the equipment to be moved to locations remote from the permanent 240V mains supply. This caravan is air-conditioned to enable reliable operation of the computer and electronics in the tropical environment in which it is used.

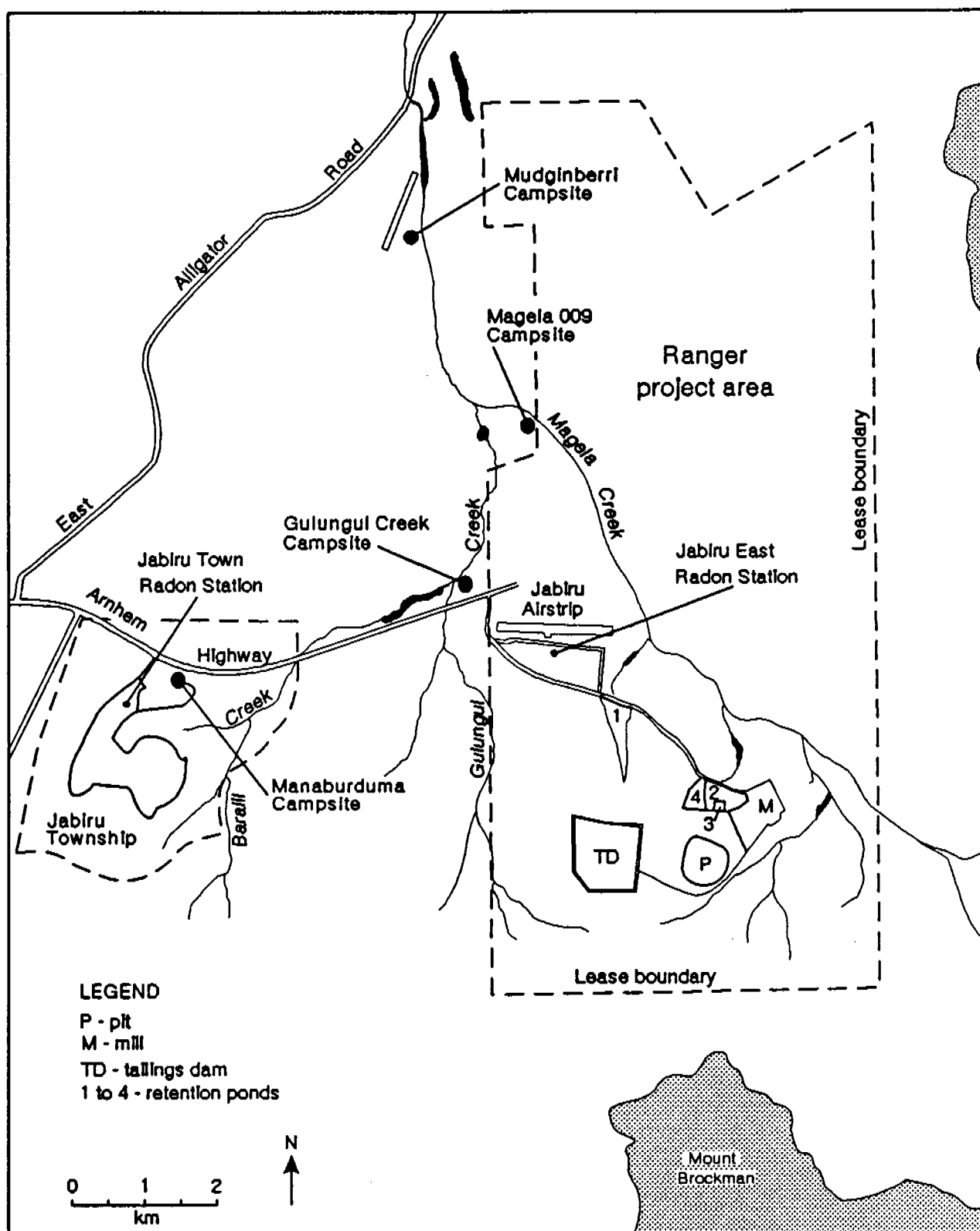


Figure 1 A locality map

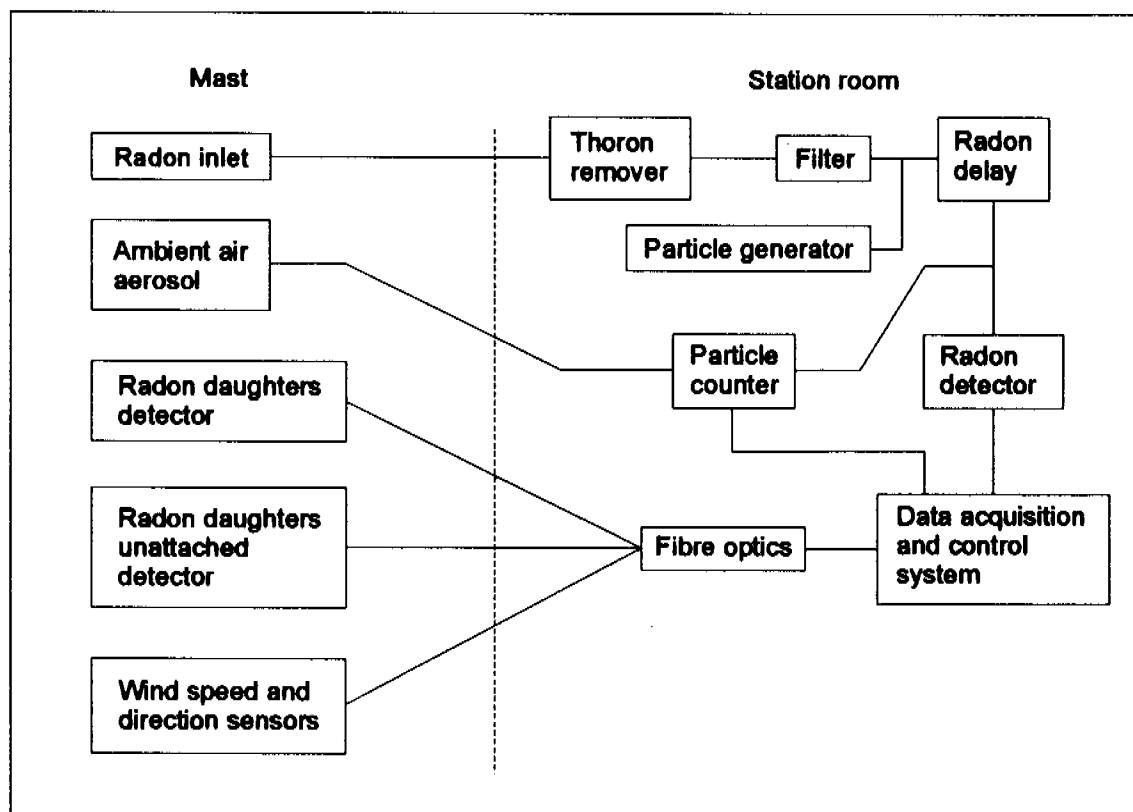


Figure 2 A block diagram of the mobile radon station equipment

## Radon detection

A high sensitivity radon detector is required to be able to detect small increases from the mine above the natural background radon concentrations. A detailed description of the theory of the detector is given by Whittlestone (1985). The essential components of the radon detector are shown in figure 2. Air is pumped continuously from the inlet through the thoron remover, delaying the gas flow by about five minutes. Since thoron has a half life of 54 s, only a small fraction of its initial concentration is likely to remain in the sampled air entering the inlet filter of the radon delay chamber. The thoron daughters and other non-gaseous radioactivity are removed by the inlet filter, leaving only radon in the chamber. While the air passes through the delay chamber, some of the radon gas decays. The resulting radon daughters become attached to the aerosol produced by a particle generator, and are retained on the outlet filter in the radon detector. The alpha particles due to radioactive decay of these daughters are counted using a silver activated zinc sulfide screen and a photomultiplier.

In practice, not all of the radon daughters produced in the delay chamber are collected on the outlet filter. The major loss is by plate-out to the walls of the chamber before attachment to a particle, and is therefore strongly dependent on the particle concentration. Too low a particle concentration results in a low efficiency. On the other hand, too high a particle concentration results in unacceptably rapid clogging of the filter. Therefore a particle counter has been incorporated into the detector system to monitor the particle concentration and permit the control computer to adjust the particle generator accordingly.

The particle generator comprises a flat nichrome wire dipping into an oil reservoir. While there is no current, the oil is drawn up the wire by capillary action. When the current heats the wire, the oil just above the surface bursts into sub-micron droplets which are carried by convection into the air stream.

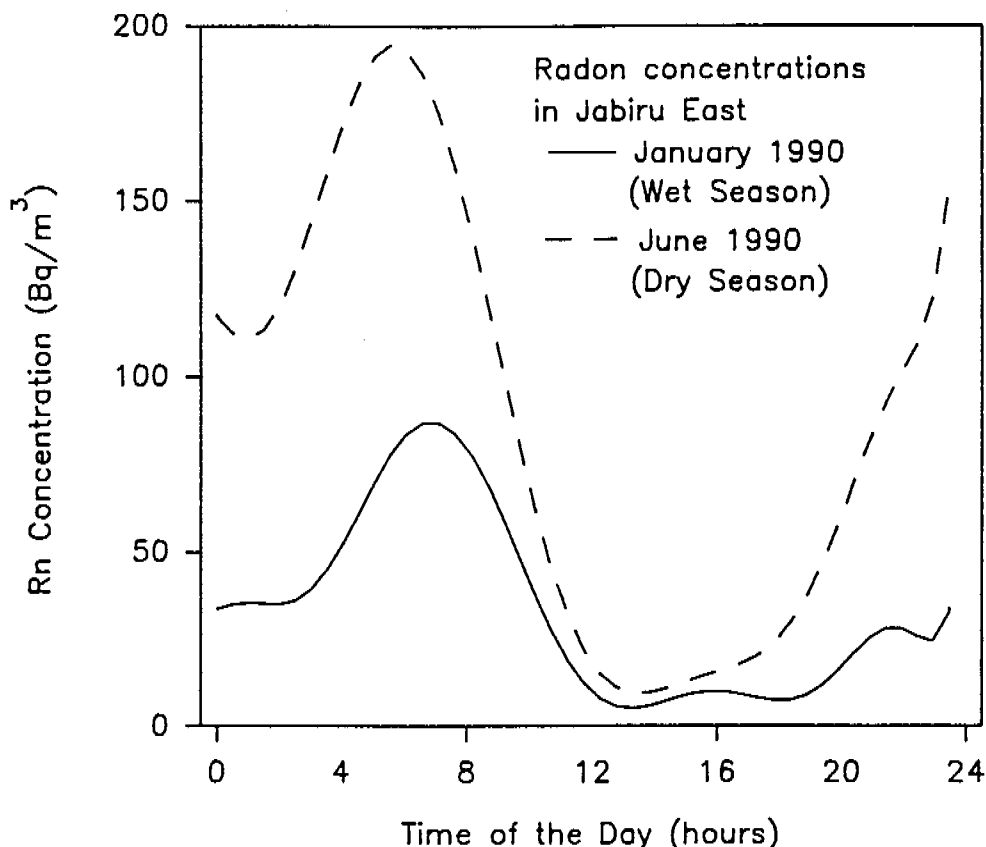


**Figure 3** Diurnal variations in average monthly radon concentrations

The particle counter is essentially a cloud chamber. The air sample is saturated with water vapour, then expanded to produce supersaturation. Condensation occurs on every particle in the sample, and each tiny water drop grows to the same size, regardless of the size of the constituents of the original particle. The amount of light scattered from a beam is, therefore a function only of the number of particles in the sample. The particle counter used at the mobile radon station has been calibrated against a standard particle counter.

Design details of the particle generator and particle counter have been described by Pfitzner and Whittlestone (1992).

The detector has a response time between 60 and 90 minutes. Allowance for this must be made when correlating the radon with the other parameters measured at the station.

Calibration of the detector is carried out by a direct method of injecting aged air with a known radon concentration derived from a solid  $^{226}\text{Ra}$  source. In addition, an indirect calibration was obtained by operating the mobile radon station for four days under ambient conditions in parallel with an independently calibrated RGM type 2 detector.

The average daily response curves for the months of January 1990 and June 1990 in Jabiru East, shown in fig 3, illustrate the generalised features of the diurnal variations of radon concentrations. Calm atmospheric conditions prevail below the atmospheric temperature inversion layers during the early hours of the day. Consequently, the radon emitted from the ground mixes slowly, and the atmospheric concentrations near the ground level increase. The atmospheric mixing conditions improve and the radon concentrations decrease during the later part of the day.

Another feature of fig 3 is the higher radon concentrations during June 1990 when compared with those during January 1990. These months typically represent the Dry and the Wet season trends respectively. The soil is generally expected to be moist during the month of

January. Also certain areas of the ground which are exposed during June, may be under water in January. Radon emission from moist to wet soils is expected to be less than that from dry soils of same  $^{226}\text{Ra}$  concentrations (Strong & Levins 1982, NCRP 1988). Additionally, the ground cover and grasses in this area are traditionally burnt with the onset of the Dry season in April-June period. This may further expose the soils and result in cracking and greater soil porosity during the Dry season. Hence sub-surface radon is expected to find an easier pathway to the atmosphere during the Dry season.

## Radon daughter detection

The ambient radon daughters are removed via air filters and detected by measuring alpha particles on a filter paper through which air is drawn (fig 2). This method does not always give an accurate measurement of actual daughter concentration, because some are beta emitters, and are not registered. Errors will occur under conditions where the ratios of the daughters are far from the equilibrium values. However, the main purpose of the measurement is to find the biologically significant radiation exposure which is almost entirely caused by the alpha particles.

The potential alpha energy concentration PAEC per litre of air is given by:

$$\text{PAEC (MeV/L)} = E_{\alpha} N_{\alpha} \quad (\text{i})$$

where  $E_{\alpha}$  is the average alpha potential energy and  $N_{\alpha}$  is the number of alpha particles emitted per litre of sampled air.  $N_{\alpha}$  can be calculated from the number of observed counts 'C' in a time interval 't' as:

$$N_{\alpha} (\text{\#}/\text{L}) = C/\eta Ft \quad (\text{ii})$$

where  $\eta$  is the detector efficiency and F, the flow rate in litres per unit time.

Calibration in terms of alpha particles per litre of air ( $N_{\alpha}$ ) is direct and accurate because a standard source is used to measure the efficiency ( $\eta$ ) of the alpha detector, and the flow rate (F) of the air is monitored by a precision flow meter. Converting the number of alpha particles to potential alpha energy ( $E_{\alpha}$ ) is less direct, because the mixture of  $\text{Po}^{218}$  (6.0 MeV) and  $\text{Po}^{214}$  (7.69 MeV) varies according to the time for ingrowth of daughters from 1:1 for very young radon in air to 1:16.2 for air in which the radon daughters have reached equilibrium. The average potential alpha energy for equilibrium air is 7.6 MeV. A reasonable lower limit for the age of radon in outdoor air is 10 minutes. The corresponding ratio of  $\text{Po}^{218}$  to  $\text{Po}^{214}$  decays in 1:2.5 which gives an average alpha energy of 7.2 MeV. If a value of 7.4 MeV is used for  $E_{\alpha}$ , the maximum error from variation of ages of ambient air is 0.2 MeV which is usually small for most public dose estimates.

A progressively decreasing number of radon daughter atoms collected in a half-hourly time interval disintegrate and emit alpha particles in the sequential time intervals. This effect needs consideration while correlating the potential alpha energy concentrations and other parameters such as wind direction. Regional data indicate that within the standard deviation of 25-40 degrees, the wind direction generally persists for time intervals longer than a half hour. Consequently the error in wind direction correlations is expected to be small. Corrections may be required for more generalised applications.

The atmospheric radon daughter concentrations closely follow the radon concentrations in air. This has been shown through the average daily response curves for the months of January 1990 and June 1990 in Jaberu East (fig 4). The corresponding relative values of radon concentrations have been produced by using the data shown in fig 3. The radon and radon daughter concentration data have been used to produce the average equilibrium factor trends which are also shown in fig 4.

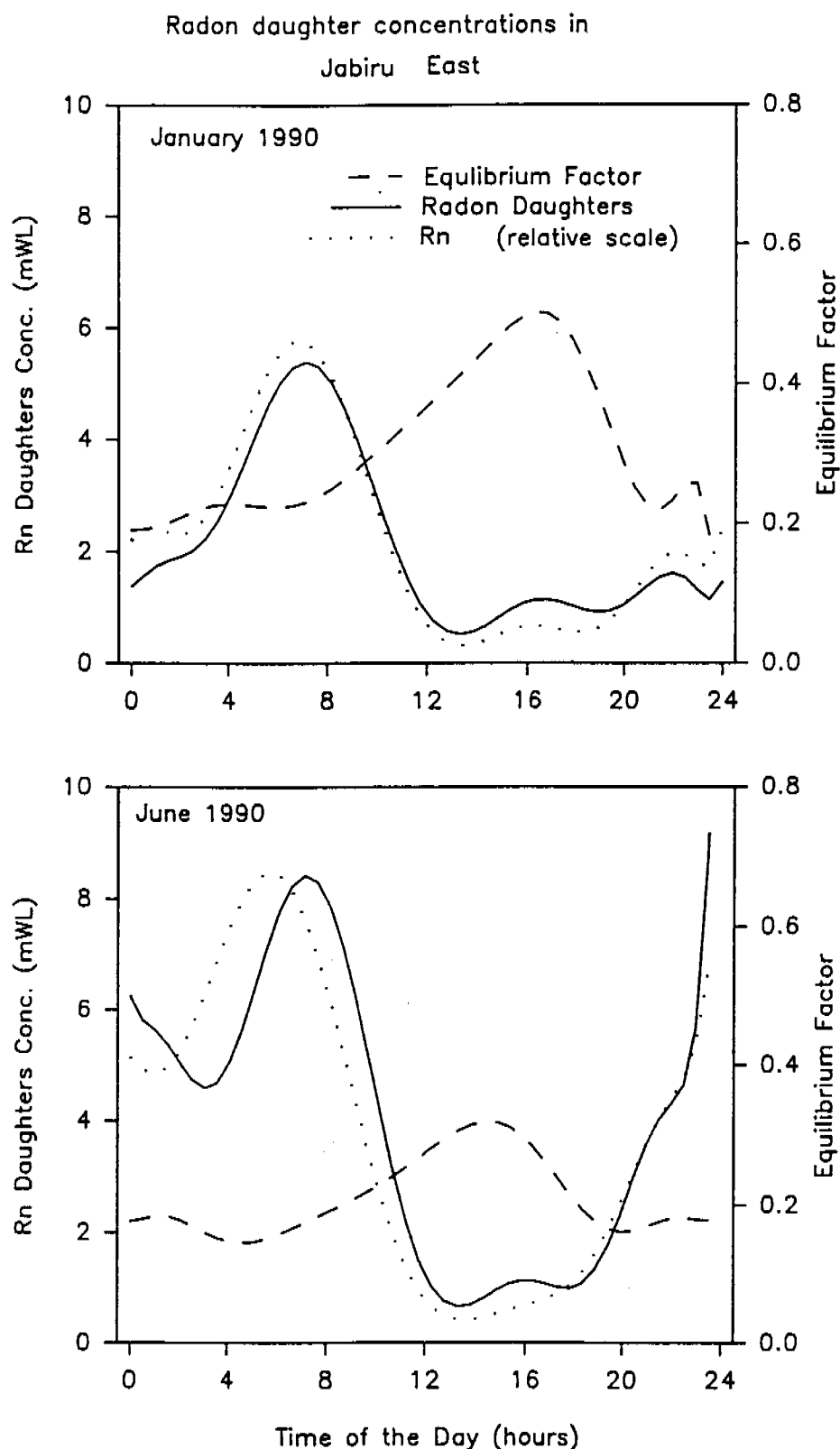


**Figure 4** Average monthly radon daughter concentrations as a function of the time of the day. The relative radon concentrations (dotted lines) are also shown for comparing the trends. The equilibrium factors (dashed lines) are calculated using half hourly radon and radon daughter concentration data.

# Jabiru East Wind Data

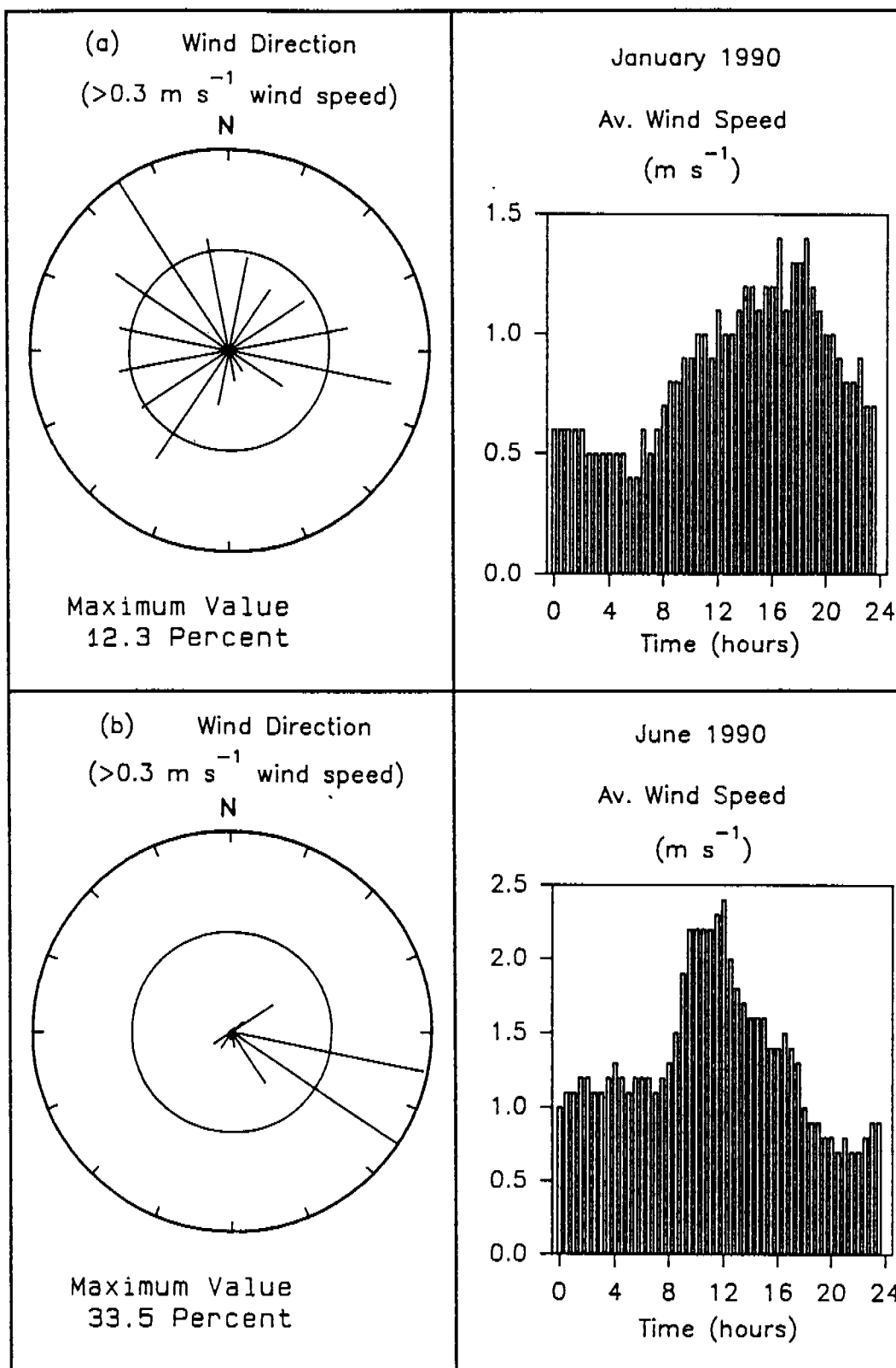


**Figure 5** The wind direction distribution in Jabiru East during the months of January and June, 1990. The left hand side of the figure shows the variations in the average wind speeds as the time of the day.



The equilibrium factor varies typically between 0.2 and 0.5 with larger values observed from about mid-day to late afternoon when the radon concentrations are low. This behaviour is probably because the predominant source of radon during the night to early morning period is local and radon is detected before it reaches equilibrium with its daughters. During the day, the radon is mixed more regionally and there is a longer period for daughter ingrowth and attachment to the ambient aerosols.

A study by Woods (1989) shows diurnal variations in the equilibrium factor measured at the tailings repository of Nabarlek uranium mine. Three sets of data were reported in that study covering periods of several days in October 1985, September 1987 and October 1988. The time difference between the radon peak and the maximum equilibrium factor was quite variable in these data sets, with the September 1985 behaviour being similar to that observed in the present work for Jabiru East. Woods (1989) does not comment on the reported observations.

## **Meteorological parameters**

Wind speed and wind direction sensors are installed on the top of the 12 m mast. While in operation the station is parked to have minimum interference from the trees and other structures. During transport, the mast is lowered on the caravan. Minimum adjustments are required when the mast is re-erected for operation at a new location. The anemometer was supplied by Climatronics of USA. Wind direction is measured by a conventional wind vane with low friction ball bearings and potentiometer. The starting speed of the anemometer and the wind vane is less than  $0.3 \text{ ms}^{-1}$ .

Power supply and signal processing electronics for the meteorological equipment are situated on the tower. Signals are converted into light pulses for transmission to the data logger via optical fibre cables. This is a precaution against damage in the event of a direct or close lightning strike.

Strong seasonal variations occur in the wind behaviour in this area (Natmap 1986, Clark 1977, et al 1993). The wind data in fig 5 show some general regional features for the Wet (November–March) and the Dry (May–September) seasons. The ESE–SE trend prevails during the Dry season. Monsoonal winds blow from the NW to NNW during the Wet season, but the trend is not as persistent as for the ESE–SE winds during the Dry season.

## **Correlation between radon concentrations and wind speed**

Radon concentrations show a broad inverse correlation with wind speed (fig 6). A probable explanation for this correlation is the dispersion of radon in a larger volume due to vertical mixing under unstable atmospheric conditions. Diurnal variations are observed both in the radon concentrations and the wind speed (fig 3 & 5). Riley (1989) points out that near the ground level stable conditions prevail after the sunset, but a low-level wind speed maximum develops at near 1 km altitude. After sunrise this maximum convectively mixes down to the ground level and hence higher wind speeds are noticed during the day time. A second smaller peak appears in the Dry season wind speed during the night. It is most probably associated with the sea-breeze from the coastal line about 60km due North (Clark et al 1993).

## **Correlation between radon concentrations and wind direction**

Correlations between the radon/radon daughter concentrations and wind direction are required in assessing the contribution of mine derived sources to the radiation dose at a sampling point. The correlations for January and June 1990 when the mobile station was parked in Jabiru East are shown in fig 7. The data are sorted into sixteen  $22\frac{1}{2}^\circ$  wind sectors. Starting clockwise from the north, the mine related sources are located in sectors 6, 7 and 8 relative to the sampling location in Jabiru East. The higher values in these sectors demonstrate that the instruments are capable of resolving the mine related signal from the background signal a few kilometres away from the mine site. Some spread of the signal to the adjacent sectors is also expected. This is because the standard deviation in wind direction of half-hourly readings is large, typically between  $30^\circ$  and  $40^\circ$ .

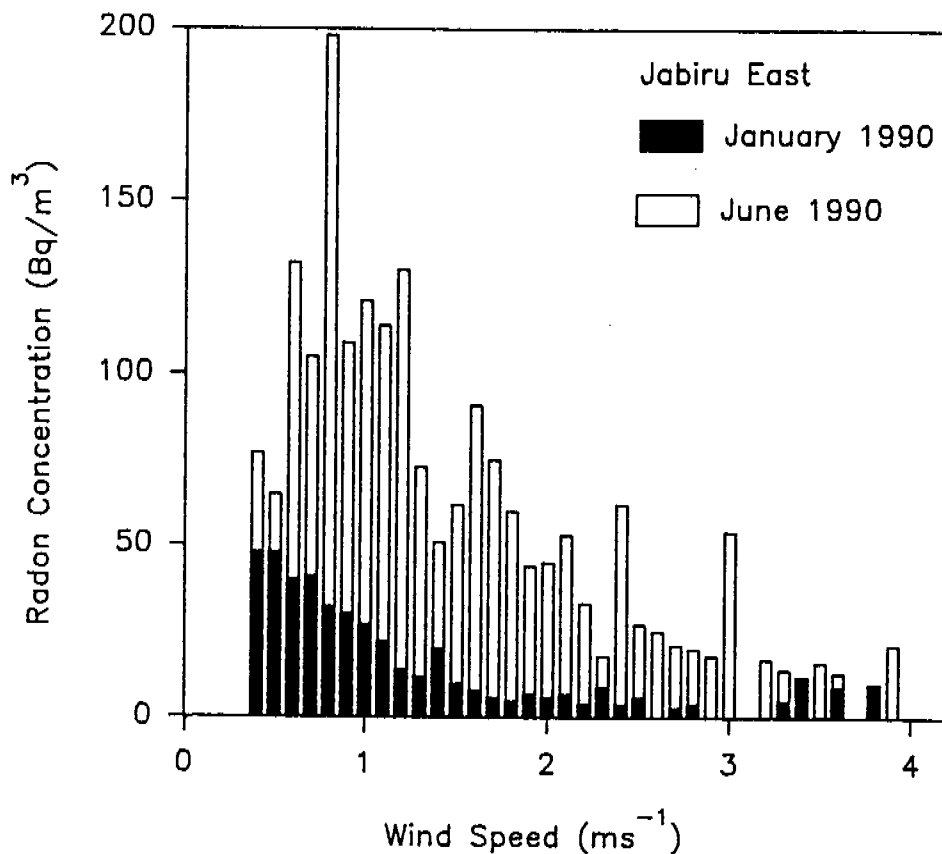


Figure 6 Radon concentrations vs. wind speed for the January 1990 and June 1990 (overlay)

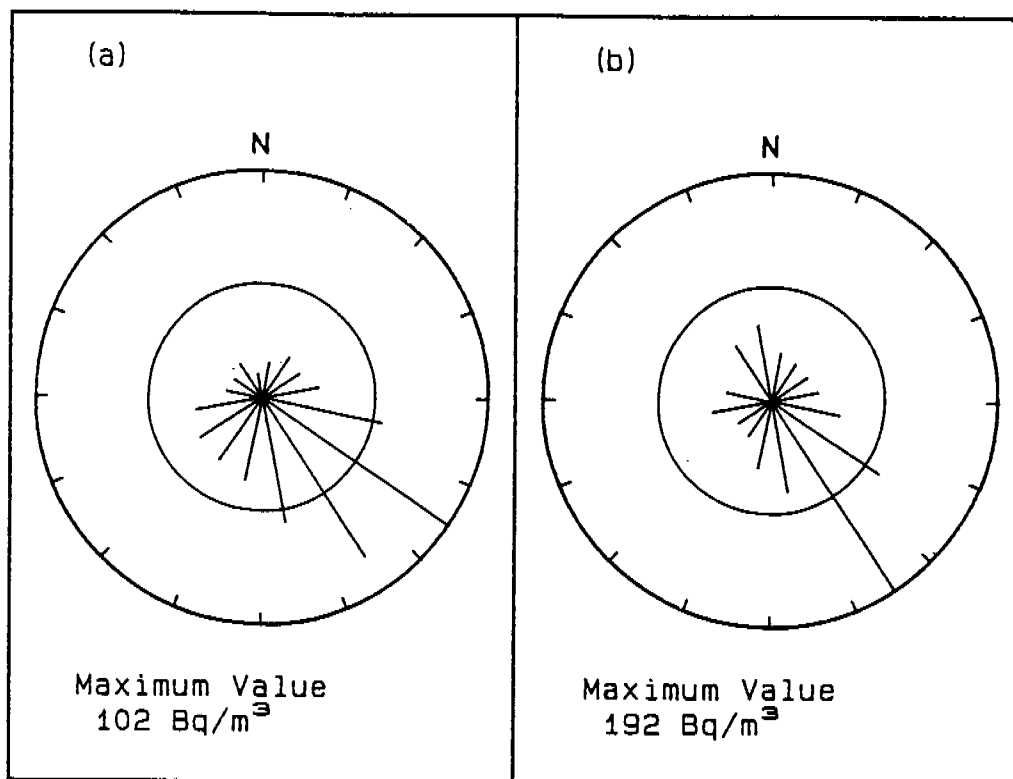


Figure 7 Radon concentrations in different wind sectors in Jabiru East  
(a) January 1990 and (b) June 1990

Additionally, curvature in the radon plume movement profiles can occur due to local meteorological conditions. This effect has also been observed during smoke plume experiments conducted in this area (to be reported). Local convective cells are formed soon after the sunrise which create localised artefacts in plume trajectories. Plume experiments also showed that little entrainment takes place within the arboreal canopy.

The actual public dose estimates using radon concentrations and wind direction data require more parameters to be considered. For example, our observations show that the distinguishable differences in radon concentrations in mine-related and background sectors occur mainly during the early morning peaks. Differences in the wind frequencies during different times of the day, therefore, need to be considered (Akber et al 1991).

### Vertical variations in radon concentrations

As mentioned earlier the detection system of the mobile station can be fixed on a detached support to sample from a height of 2 m or lower. Two sets of simultaneous measurements were conducted at 15 m and 2 m heights when the mobile station was located beside the fixed station in Jabiru. The results shown in table 1 are the average values for the half-hourly radon and radon daughter concentrations and their ratios. Initially the 2 m equipment was located outdoors; later it was moved inside the fixed monitoring station building which is a well-ventilated, air-conditioned, metal-clad, high-set demountable.

For outdoor measurements, both radon and radon daughter concentrations at 2 m are higher than those at 15 m, although the standard deviations of the ratios are large. Also, the radon concentration ratio is higher than the radon daughter concentration ratio. Hence it may be that a larger proportion of the freshly emitted radon is sampled by the detectors near the ground level. This, in turn, would result in higher radon concentrations with proportionately lesser concentrations of radon daughters due to less available time for the build up.

Comparison of results from 15 m outdoor and 2 m indoor show different behaviour of radon and radon daughter concentrations. The radon concentrations have a ratio similar to that for the outdoor measurements but the indoor to 15 m outdoor radon daughter concentrations ratio is lower. This can be explained by the fact that the forced air exchange due to ventilation does not allow for radon daughters to build up to the level of the calm outdoor conditions. Additionally, some radon daughters are likely to plateout to the air-conditioner filter system. This result should be generalised with some caution for the Jabiru dwellings which are mostly well-sealed brick houses. Another study in Jabiru houses shows that outdoor and indoor radon daughter concentrations are variable, but the average of the indoor and outdoor measurements are comparable to each other (Kvasnicka 1990).

Radon and radon daughter concentration averages in table 1 have a large standard deviation. This is due to the already discussed large variability in the signal at various times of the day.

**Table 1** Vertical variations in radon and radon daughter concentrations. Data are for Jabiru Town.

Time period	Measurement height	Radon (Bq/m <sup>3</sup> )		Radon daughters (mWL)	
		Value	Std dev	Value	Std dev
25 Aug–4 Sept 1989	2 m (outdoors)	25	22	2.8	2.0
	15 m	20	19	2.4	1.8
	Ratio	1.4	0.5	1.2	0.3
4 Sept–21 Sept 1989	2 m (indoors)	35	37	1.9	2.1
	15 m	25	37	2.8	3.2
	Ratio	1.6	0.6	0.8	0.2

## **Acknowledgments**

Dr A Johnston contributed during the early stages of the project. Mr R Marten, Mr B Barrowcliff and Mr M Davy helped in commissioning the station.

## Determination of $^{227}\text{Ac}$ by alpha-particle spectrometry

G Hancock, P Martin and RA Akber

---

### Abstract

A method is described for the determination of  $^{227}\text{Ac}$  concentrations in environmental samples. Actinium is separated from the sample digest by co-precipitation with lead sulphate, purified using anion and cation exchange techniques, and electrodeposited onto a stainless steel disc. The chemical yield is monitored by addition of a  $^{229}\text{Th}/^{225}\text{Ra}/^{225}\text{Ac}$  tracer before sample dissolution.  $^{225}\text{Ac}$  recovery is determined from an initial count by measurement of its alpha emitting daughter,  $^{217}\text{At}$ . The disc is then stored for two to three months and recounted. The  $^{227}\text{Ac}$  activity is obtained by measurement of the ingrown  $^{227}\text{Th}$  and  $^{223}\text{Ra}$  activities in the 5.38–6.10 MeV region. Co-precipitation with lead sulphate enables the convenient determination of actinium, thorium and radium on the same sample digest.

---

### Introduction

$^{227}\text{Ac}$  is a member of the  $^{235}\text{U}$  series, and a parent of  $^{227}\text{Th}$  and  $^{223}\text{Ra}$ . This series is only naturally present as 4.6% of the activity of the  $^{238}\text{U}$  series, and so the  $^{227}\text{Ac}$  activity in most environmental samples is extremely low. However, the radiotoxicity of  $^{227}\text{Ac}$  is high, and the annual radioactivity limits of ingestion are a factor of 80 lower than  $^{238}\text{U}$ , and a factor of 10 lower than  $^{226}\text{Ra}$  (ICRP 1991). Hence the detection of low levels of  $^{227}\text{Ac}$  in environmental samples is sometimes required.

In addition, the measurement of  $^{227}\text{Ac}$  has been used to indicate the source of  $^{223}\text{Ra}$  in groundwaters (Dickson 1985, Martin & Akber 1994 [this publication]). As a naturally occurring homologue of trivalent man-made transuranic elements, it has also been suggested as a means of studying their comparative geochemical behaviour (Bojanowski et al 1987).

Alpha-particle spectrometry is a particularly sensitive technique for the determination of  $^{227}\text{Ac}$ . Although a beta-emitter, it can be determined indirectly via measurement of its alpha-emitting daughters,  $^{227}\text{Th}$  and  $^{223}\text{Ra}$ . Anderson & Fleer (1982) and Nozaki (1984) chemically isolated actinium, and then separated and measured  $^{227}\text{Th}$  after a suitable ingrowth period. Dickson (1985) determined  $^{227}\text{Ac}$  by measurement of the  $^{223}\text{Ra}$  activity in samples 5 months after collection.

Bojanowski et al (1987) electrodeposited actinium onto a stainless steel disc and measured the integrated  $^{227}\text{Th}$  and  $^{223}\text{Ra}$  activity after an ingrowth period of 2–3 months. This technique

gives at least a twofold gain in sensitivity over the individual determination of  $^{227}\text{Th}$  or  $^{223}\text{Ra}$ . In their method, actinium was separated from the sample digest by preconcentration as oxalate and hydroxides, purified on ion-exchange columns and electrodeposited.  $^{225}\text{Ac}$  was used as a yield tracer.

The method described here uses lead sulphate to co-precipitate actinium, radium and thorium. Actinium is then separated from radium and thorium on an anion exchange column, purified on a cation exchange column and electrodeposited from an aqueous/ethanol solution. The use of lead sulphate precipitation as a preconcentration technique following the addition of a  $^{229}\text{Th}/^{225}\text{Ra}/^{225}\text{Ac}$  tracer enables the convenient determination of actinium, radium and thorium on the same sample digest (Martin & Hancock 1994).  $^{225}\text{Ac}$  recovery is determined from an initial count by measurement of its alpha-emitting daughter,  $^{217}\text{At}$ . The disc is then recounted 2–3 months later, and the  $^{227}\text{Ac}$  activity obtained by measurement of the ingrown  $^{227}\text{Th}$  and  $^{223}\text{Ra}$  activities in the 5.38–6.10 MeV region. Chemical yields are typically 70–75%.

## Methods

### Chemical procedures

- 1 Add the required amount of tracer, and dissolve the sample using an appropriate technique. Evaporate to dryness and bring the residue into solution in 100 mL 0.1 M HCl or  $\text{HNO}_3$ .
- 2 Add 1 mL of 98%  $\text{H}_2\text{SO}_4$ , 2 g  $\text{K}_2\text{SO}_4$  and dissolve. Add 1 mL 0.24 M  $\text{Pb}(\text{NO}_3)_2$  solution drop-wise whilst stirring. Heat, allow the precipitate to settle, and decant the supernatant when cool. Wash with 20 mL 0.1 M  $\text{K}_2\text{SO}_4/0.2$  M  $\text{H}_2\text{SO}_4$  solution and decant again.
- 3 Add 5 mL 0.1 M ammoniacal EDTA solution (pH 10), and 2 drops ammonia to the  $\text{PbSO}_4$  precipitate, and warm the beaker to aid dissolution. If necessary add further 1 mL portions of EDTA solution until the precipitate has dissolved. Pass the solution through an anion exchange column (Bio-Rad AG1-X8, 100–200 mesh, Cl form, 80 mm height, 7 mm i.d.), and wash with 13 mL 0.005 M EDTA/0.1 M ammonium acetate at pH 8. Thorium and actinium are retained on the column; radium is eluted at this stage. Elute actinium\* with 25 mL 8 M  $\text{HNO}_3$ . Collect the eluate and evaporate to dryness. Dissolve the residue in a minimum volume (3–5 mL) of 2.5 M HCl.

\* Note the time ( $t_0$ ) of separation of radium and actinium.

- 4 Prepare a cation exchange column (Bio-Rad AG50W-X8, 200–400 mesh, H form, 80 mm height, 7 mm i.d.), and wash with 15 mL 2.5 M HCl. Pour the solution containing the actinium fraction onto the column, and wash with further 2 mL aliquots of 2.5 M HCl until a total of 10 mL has been added. Wash the column with 30 mL 3 M  $\text{HNO}_3$  to elute lead and residual radium and polonium. Add a further 35 mL 3 M  $\text{HNO}_3$  to elute actinium. Collect the eluate, evaporate to a low volume, and bring to dryness at low heat.
- 5 Dissolve the residue in 1 mL 0.1 M  $\text{HNO}_3$  and transfer to a deposition cell with 9 mL ethanol. The cell is a disposable polyethylene scintillation vial as described by Talvitie (1972). The distance between cathode and anode is 4 mm.

Electrodeposit onto a stainless steel disc at 100 mA for 30 mins. Add 2 drops of ammonia 1 minute before stopping, remove the disc and allow to air-dry. The surface of the source should not be touched.

## Spectroscopy

The recovery of the  $^{225}\text{Ac}$  tracer ( $t_{1/2} = 10.0$  d) is determined from a first count commenced as soon as possible after electrodeposition (fig 1a). The  $^{225}\text{Ac}$  activity is most easily measured via its grand-daughter  $^{217}\text{At}$  at 7.06 MeV, which is in secular equilibrium. The disc is then stored for 2–3 months to allow decay of  $^{225}\text{Ac}$  and ingrowth of  $^{227}\text{Th}$  and  $^{223}\text{Ra}$ , and recounted (fig 1b). The activity in the 5.38–6.10 MeV energy region is due to  $^{227}\text{Th}$ ,  $^{223}\text{Ra}$  (99.4%), plus any remaining  $^{225}\text{Ac}$  activity to be deducted from this region.

Although radium, polonium and thorium should have been completely removed during the chemical separation procedures, a check should be made for their presence. Any  $^{222}\text{Rn}$  (5.49 MeV) and  $^{218}\text{Po}$  (6.00 MeV) which may be present due to the decay of  $^{226}\text{Ra}$  can be stripped by deducting twice the activity of the  $^{214}\text{Po}$  peak at 7.68 MeV. Potential interference from  $^{210}\text{Po}$  (5.30 MeV) was avoided by routinely choosing 5.38 MeV as the lower energy limit for  $^{227}\text{Th}$  and  $^{223}\text{Ra}$  measurement. The resultant loss of measurable activity in the 5.25–5.38 MeV region due to  $^{223}\text{Fr}$  at 5.34 MeV and  $^{223}\text{Ra}$  (0.6%), is less than 1% of the total  $^{227}\text{Th}$  and  $^{223}\text{Ra}$  activity.

$^{228}\text{Th}$  and its daughters  $^{224}\text{Ra}$  and  $^{212}\text{Bi}$  are the major potential interferences, and their contribution to the  $^{227}\text{Th}$  and  $^{223}\text{Ra}$  area cannot be measured quantitatively. However, their presence can be detected via measurement of the  $^{212}\text{Po}$  peak at 8.78 MeV.

## Calculation of $^{227}\text{Ac}$ activity

98.62% of the  $^{227}\text{Ac}$  activity decays by beta emission to  $^{227}\text{Th}$ , and 1.38% by alpha-particle emission to  $^{223}\text{Fr}$  (fig 2). 100% of  $^{227}\text{Th}$  and 99.4% of  $^{223}\text{Ra}$  decays result in alpha-particle energies in the 5.38–6.10 MeV region (Lederer & Shirley 1978).

Hence the  $^{227}\text{Ac}$  activity at the time of separation  $t_0$ , for a disc counted at any time  $t$  after separation, is given by:

$$A^0_{\text{Ac}} = \frac{A_m}{0.9862 I_{\text{Th}}(t) + 0.994 I_{\text{Ra}}(t)}$$

where  $A_m$  is the measured ( $^{227}\text{Th} + ^{223}\text{Ra}$ ) activity; and  $I_{\text{Th}}(t)$  and  $I_{\text{Ra}}(t)$  are the calculated ingrowth fractions at time  $t$  for  $^{227}\text{Th}$  and  $^{223}\text{Ra}$  respectively.

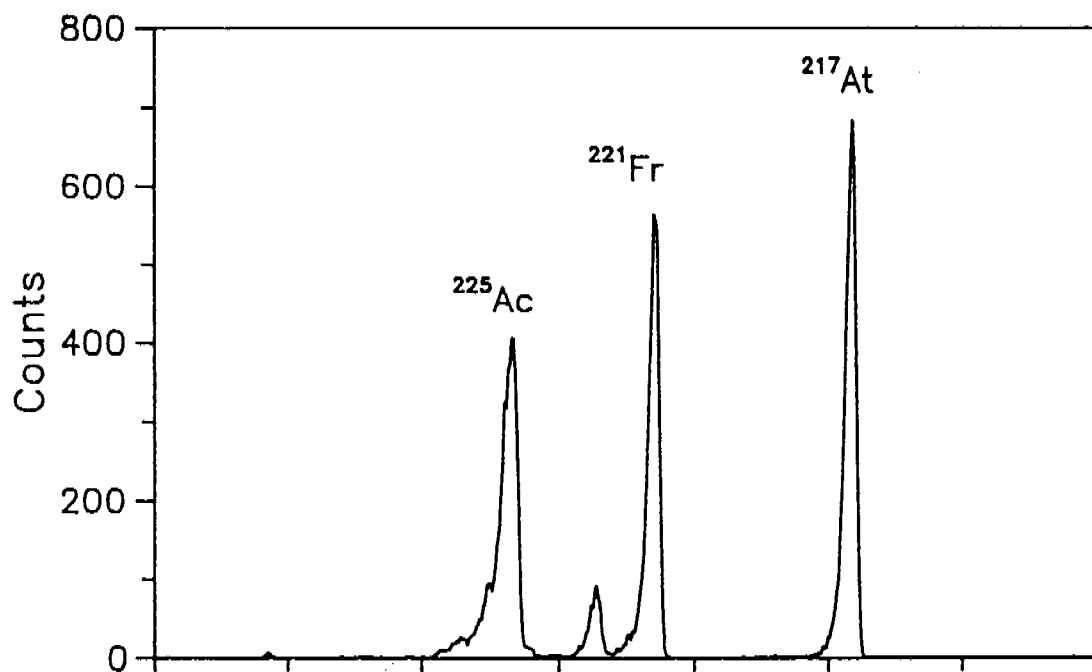
---

## Discussion

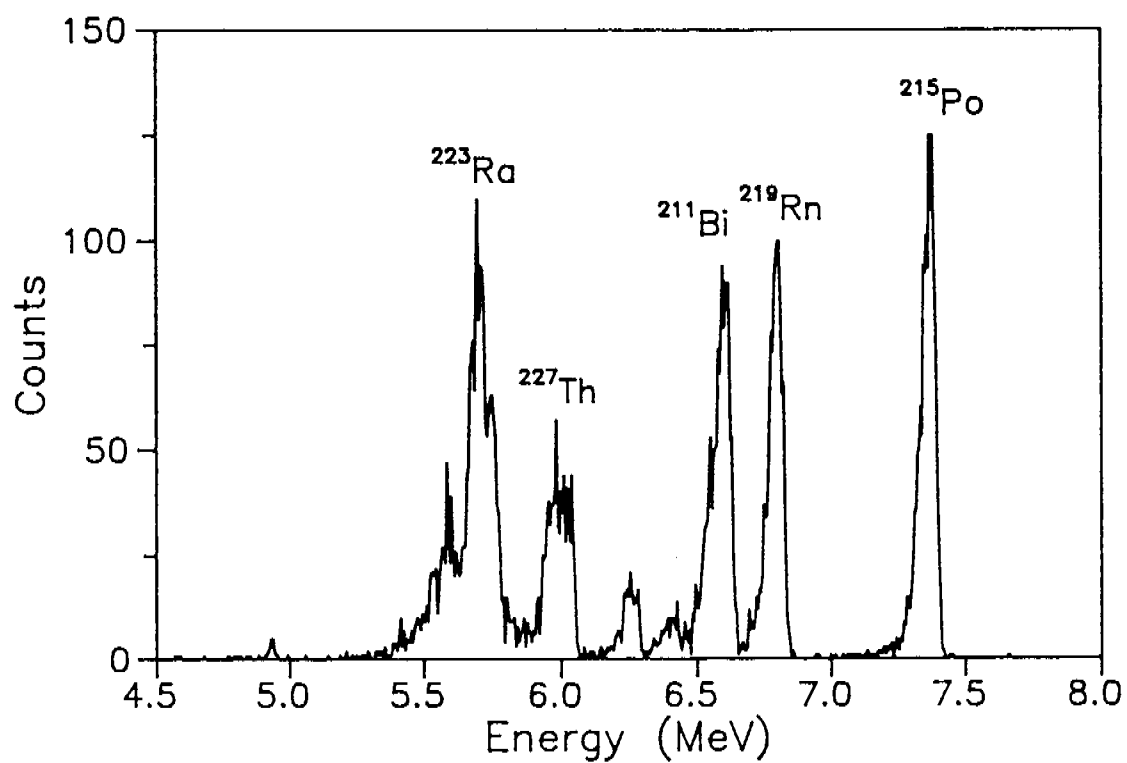
### Tracer

The quantity of  $^{225}\text{Ac}$  tracer added will depend largely on how soon the  $^{227}\text{Ac}$  determination is required. Figure 3 shows the relative ingrowth and decay curves for  $^{227}\text{Th} + ^{223}\text{Ra}$ , and  $^{225}\text{Ac}$ . If a determination of  $^{227}\text{Ac}$  within 2 months is required, the quantity of  $^{225}\text{Ac}$  added should be limited so that the  $^{225}\text{Ac}$  activity present in the final count is small compared to the integrated  $^{227}\text{Th}$  and  $^{223}\text{Ra}$  activity.

As the tracer is added as a  $^{229}\text{Th}/^{225}\text{Ra}/^{225}\text{Ac}$  solution, Steps 2 and 3 in the chemical procedures should be performed as soon as possible after each other (ie within a few hours). This will minimise the effect of any differences in the efficiency with which thorium, radium and actinium are carried in the lead sulphate lattice.

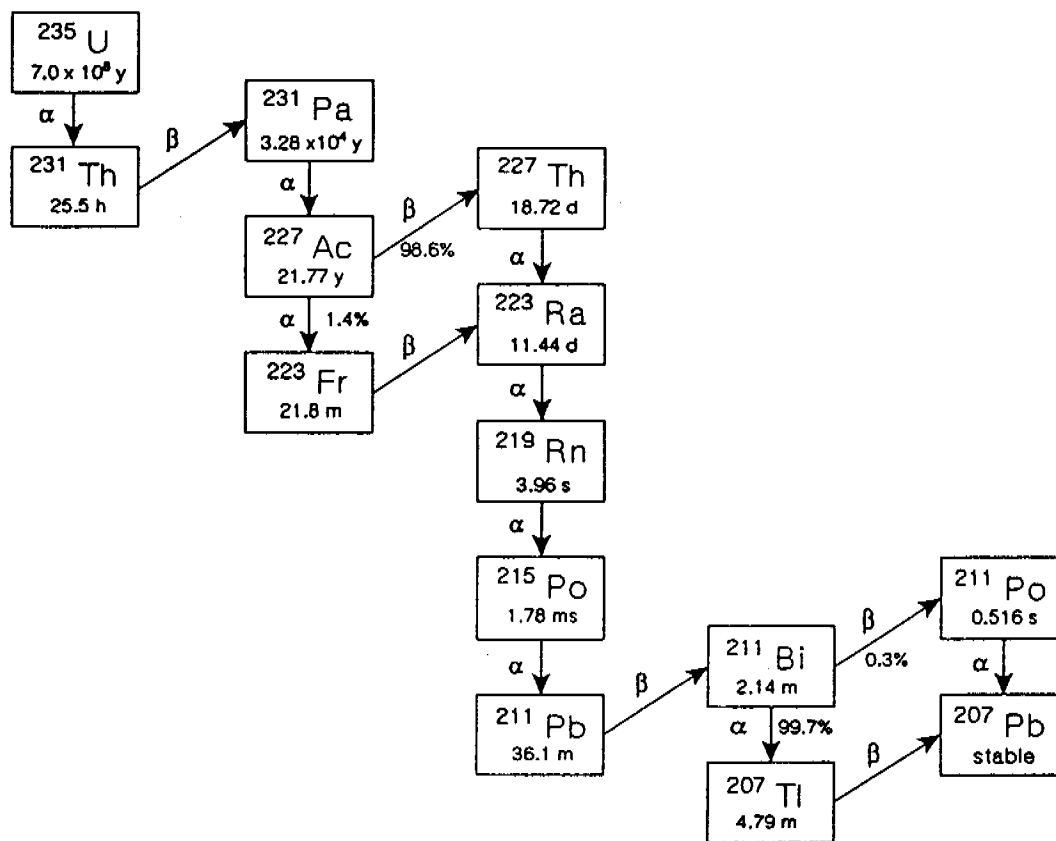
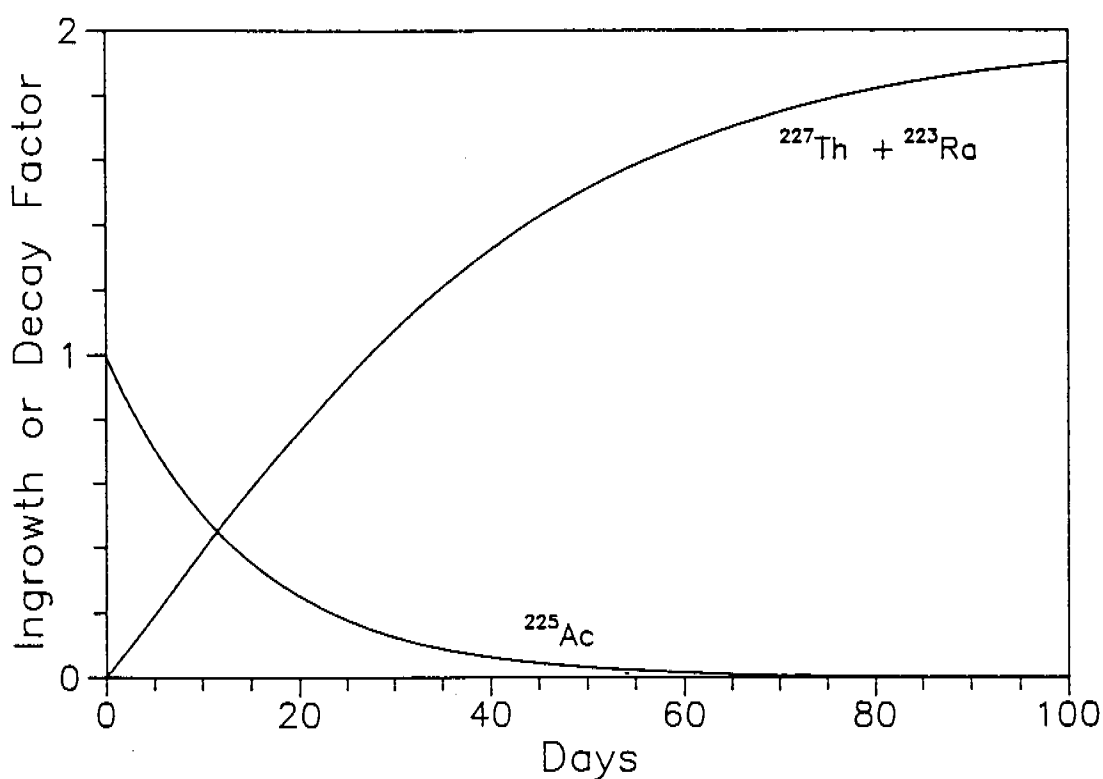


**Figure 1a** An actinium source counted immediately after electrodeposition



**Figure 1b** The same source counted three months later




 Figure 2 The  $^{235}\text{U}$  decay series

 Figure 3  $^{227}\text{Th} + ^{223}\text{Ra}$  ingrowth and  $^{225}\text{Ac}$  decay from an initially pure actinium source

## Removal of interferences

Actinium is separated from the sample matrix by co-precipitation with lead sulphate in the presence of potassium. Thorium and radium are also precipitated, whereas uranium remains in solution. Thorium, lead (Schönfeld et al 1958) and actinium form anionic EDTA complexes and are adsorbed onto the anion exchange column. Radium passes through the column and can be collected for analysis (Hancock & Martin 1991). Actinium is eluted with 8 M HNO<sub>3</sub>; thorium remains on the column. After evaporation of the eluate, a substantial quantity of residue is present, probably due mostly to lead and rare earth sulphates. This residue was found to be insoluble in nitric acid; however it dissolved with heating in a few mL of 2.5 M HCl. After adsorption of this solution onto a cation exchange column, elution with nitric acid (Bojanowski et al 1987) is employed. The first 30 mL wash with 3 M HNO<sub>3</sub> elutes lead, rare earth elements, polonium and any residual radium and uranium. Actinium is eluted in the following 35 mL portion. Any residual traces of thorium are retained on the column.

This separation technique gives a final actinium fraction which, after evaporation to dryness, should be virtually free of visual residue.

---

## Summary

The method described above can produce a high resolution source suitable for the determination of <sup>227</sup>Ac by alpha-particle spectrometry. Any environmental sample that can be chemically digested and brought into solution at pH 1 can be analysed. Co-precipitation with lead sulphate is a convenient method of pre-concentrating actinium, thorium and radium. The <sup>227</sup>Ac detection limit is typically 0.2 mBq/sample for a counting period of 3 days. Work is proceeding on refining the anion exchange step to allow a better separation at this point of actinium from other elements, particularly lead.

# A method for the determination of all radium isotopes in groundwaters by alpha-particle spectrometry<sup>1</sup>

G Hancock and P Martin

---

## Abstract

A method is described for the preparation of a high resolution source suitable for the determination of all natural radium isotope concentrations in groundwater samples.  $^{225}\text{Ra}$  is used as a yield tracer. The radium is co-precipitated with lead sulphate, purified using ion exchange techniques, and electrodeposited from an aqueous/ethanol solution. The radiochemical separation and electrodeposition procedures can be completed in approximately six hours. Tracer recoveries are typically 80%, and the resolution obtained is typically 40 keV FWHM.  $^{223}\text{Ra}$  and  $^{224}\text{Ra}$  are determined from their daughter products after correcting for differential radon loss.

---

## Introduction

Most analyses of radium activity concentrations in waters have focussed on  $^{226}\text{Ra}$ , and more recently  $^{228}\text{Ra}$ . This is because dose rate calculations for radium in drinking water supplies are dominated by these isotopes due their long half-lives. However, measurement of all four naturally occurring radium isotopes in groundwaters has been suggested as a useful geochemical exploration tool (Dickson et al 1983), and may also be applied to studies of radium mobilisation in saline seepages (Dickson 1985, Martin & Akber 1994 [this publication]). Unfortunately, developments in these fields have often been hampered by difficulties in the measurement of these isotopes in waters, particularly  $^{223}\text{Ra}$ ,  $^{224}\text{Ra}$  and  $^{228}\text{Ra}$ .

Common techniques for the determination of radium include direct gamma-ray spectrometry, radon emanation, liquid scintillation, and alpha-particle spectrometry following radiochemical separation. In principle, the use of alpha-particle spectrometry offers a number of advantages over alternative methods<sup>1</sup>, including:

- higher sensitivity resulting from the observation of the high-yield alpha decay process, low intrinsic detector backgrounds and the elimination of competing radiation by chemical processing,

---

<sup>1</sup> The method described in this paper is a modification of that described by Hancock & Martin (1991). Additional data are presented.

- internal calibration of the overall measurement efficiency for each sample processed through the use of isotopic tracers,
- the ability to measure concentrations of  $^{226}\text{Ra}$  without an ingrowth period for  $^{222}\text{Rn}$  and daughters, and
- the ability to measure concentrations of all the radium isotopes, including  $^{228}\text{Ra}$  if a suitable ingrowth period is allowed.

However, problems inherent in chemically isolating radium from other Group II elements (calcium, strontium, barium) in the alpha-particle spectrometry methods often result in erratic chemical yields, a poorly resolved spectrum, and/or the use of lengthy labour-intensive analytical techniques. The method reported here has been developed to overcome these problems.

Commonly,  $^{226}\text{Ra}$  concentrations have been determined by spectral analysis of a thin layer of  $\text{Ba(Ra)SO}_4$  (Sedlet 1966). Using a refined  $\text{Ba(Ra)SO}_4$  precipitation technique, Sill (1987) reported a resolution of 60 keV FWHM for a sample containing a limited quantity ( $\sim 100\text{ }\mu\text{g}$ ) of barium;  $^{133}\text{Ba}$  was used as a yield tracer for radium. If a determination of all radium isotopes is required, a spectrum with high resolution is necessary to minimise peak overlap and enable the use of spectral stripping techniques for accurate measurements of  $^{223}\text{Ra}$  and  $^{224}\text{Ra}$ . In addition, it is preferable to use as tracer an isotope of radium itself rather than a chemical analogue such as barium.

The addition of  $^{223}\text{Ra}$  or  $^{224}\text{Ra}$  as tracers (Koide & Bruland 1975, Short 1986) obviously precludes the determination of their original activities in the sample. Smith and Mercer (1970) described the use of  $^{225}\text{Ra}$  as a tracer. This isotope has the advantage that it does not occur naturally and is, therefore, not present in environmental samples. Although a beta-emitter, its activity can be calculated from the ingrowth of its alpha-emitting daughters.

The method described here can measure all alpha-emitting radium isotopes ( $^{226}\text{Ra}$ ,  $^{224}\text{Ra}$ ,  $^{223}\text{Ra}$ ) and, after a suitable ingrowth period,  $^{228}\text{Ra}$  on a single source. The separation and electrodeposition of radium can be comfortably completed in six hours, with an operator time of 30–45 minutes per sample for a batch of 4–6 samples. With the use of  $^{225}\text{Ra}$  as a yield tracer,  $^{226}\text{Ra}$ ,  $^{224}\text{Ra}$ , and  $^{223}\text{Ra}$  are determined from an initial count immediately after deposition, and from the calculated  $^{225}\text{Ra}$  recovery determined after a suitable ingrowth period for  $^{225}\text{Ac}$  and daughters.  $^{228}\text{Ra}$  is determined after an ingrowth period for  $^{228}\text{Th}$  and  $^{224}\text{Ra}$ . The resolution obtained is typically  $\sim 40\text{ keV}$ , and chemical recoveries are typically in the range 75–85%.

---

## Methods

The groundwater samples were collected in acid-washed polypropylene containers, and filtered in the laboratory through a  $0.45\text{ }\mu\text{m}$  membrane filter. Filtration, and the commencement of the chemical separation procedures generally occurred within 2–3 hours of sample collection.

## Chemical procedures

The chemical separation scheme is shown in fig 1, and described below.

- 1 Add the required amount of tracer to approximately 1 L of the filtered sample. The amount of nitric or hydrochloric acid added to the sample should be limited so that the sample acid concentration does not exceed 0.1 M.
- 2 Add 10 mL of 98%  $\text{H}_2\text{SO}_4$ , 10 g  $\text{K}_2\text{SO}_4$  and dissolve. Add 2 mL 0.24 M  $\text{Pb}(\text{NO}_3)_2$  solution drop-wise whilst stirring. Heat, allow the precipitate to settle, and decant the supernatant when cool. Wash with 50 mL 0.1 M  $\text{K}_2\text{SO}_4/0.2\text{ M H}_2\text{SO}_4$  solution and decant again.

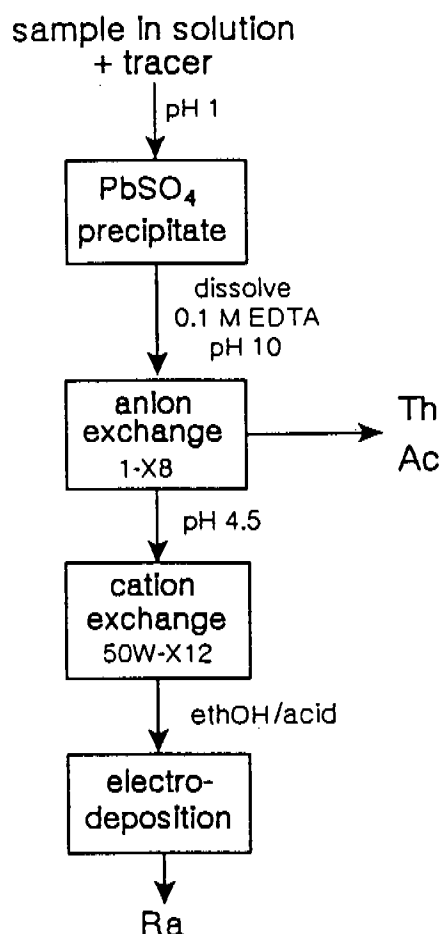


**Figure 1** Flow diagram for the radiochemical separation of radium

- 3 Add 5 mL 0.1 M ammoniacal EDTA solution (pH 10), and 2 drops ammonia to the Pb(Ra)SO<sub>4</sub> precipitate, and warm the beaker to aid dissolution. If necessary add further 1 mL portions of EDTA solution until the precipitate has dissolved. Pass the solution through an anion exchange column (Bio-Rad AG1-X8, 100–200 mesh, chloride form, 80 mm height, 7 mm i.d.) to remove sulphate, and wash with 13 mL 0.005 M EDTA/0.1 M ammonium acetate at pH 8. Thorium\* and actinium are also retained on the column. Collect the eluate in a beaker containing 1 mL 0.5 M ammoniacal EDTA and 0.5 mL 5 M ammonium acetate. Adjust the pH to 4.5 with 6 M HNO<sub>3</sub> using bromocresol green as an indicator. The final volume should be about 20 mL.

\* Record the time of thorium/radium separation.

- 4 Prepare a cation exchange column (Bio-Rad AG50W-X12, 200–400 mesh, 60 mm height, 7 mm i.d.) in the ammonium form by washing with 15 mL 1.5 M ammonium acetate, followed by 15 mL 0.20 M ammonium acetate solution previously adjusted to pH 4.5 with HNO<sub>3</sub>. The flow rate is 0.8–1.0 mL/min, and can be obtained by fitting a Luer tubing adapter and raising the column to the required height. Transfer the solution from step 3 onto the column and wash with 35 mL 1.5 M ammonium acetate in 0.1 M HNO<sub>3</sub> to elute residual lead, thorium and actinium. Add 2.5 M HCl\* in three 14 mL aliquots to wash the ammonium acetate out of the column, and elute barium. Radium is then eluted with 20 mL 6 M HNO<sub>3</sub>. Evaporate the solution to a low volume, and bring to dryness at low heat.

\* Record the time <sup>225</sup>Ac starts to grow in.

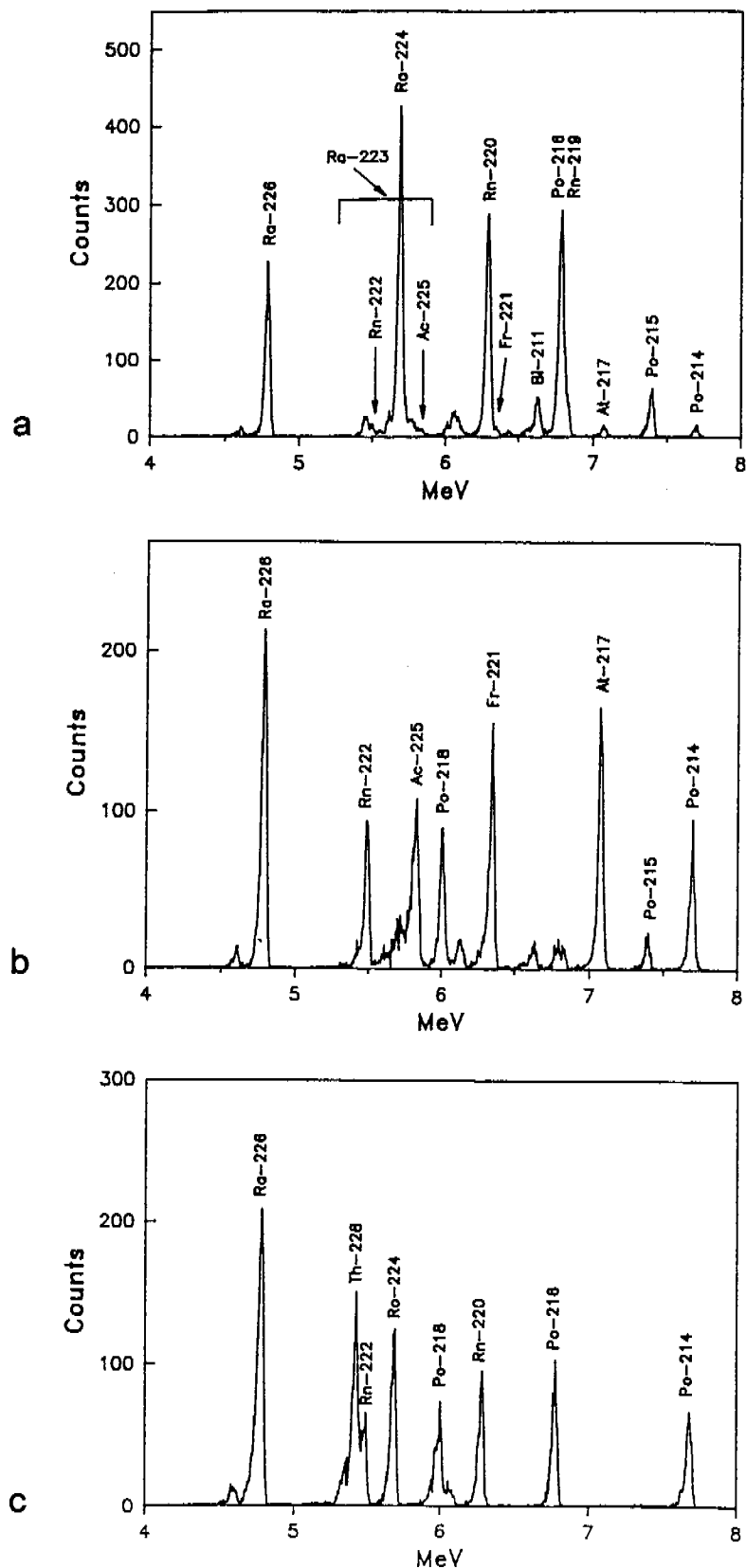


**Figure 2** a A typical groundwater sample counted immediately after deposition. 78 ksec count, FWHM of the  $^{226}\text{Ra}$  peak is 38 keV. b The same disc counted 20 days after deposition. c The same disc counted 6 months after deposition.

- 5 Dissolve the residue from step 4 in 1 mL 0.1 M HNO<sub>3</sub> and transfer to a deposition cell with 9 mL ethanol. The cell is a disposable polyethylene scintillation vial as described by Talvitie (1972). The distance between cathode and anode is 4 mm. Electrodeposit onto a stainless steel disc at 100 mA for 30 min. Add 2 drops of ammonia 1 minute before stopping, remove the disc and allow to air-dry. The surface of the source should not be touched.

## Spectroscopy

The alpha-particle spectroscopy system used consisted of a silicon surface barrier detector (450 mm<sup>2</sup> surface area) and chamber (Tennelec TC256) connected to a multi-channel analyser (Adcam 100). A negative potential of 5.6 V was applied to the source, and the chamber operated at 10–15 torr pressure to limit recoil contamination of the detector (Sill & Olson 1970). The distance between source and detector was 5–6 mm. The best peak resolution attained under these conditions for any electrodeposited source was 30 keV FWHM.

Figure 2 shows typical spectra obtained for a groundwater sample; the same disc was counted immediately after deposition (fig 2a) and then again after 20 days (fig 2b), illustrating peak positions and changes in the spectrum due to isotope ingrowth and decay. Resolution of the <sup>226</sup>Ra line is 38 keV FWHM.

Counting is commenced as soon as possible after plating in order to minimize both the decay of <sup>224</sup>Ra ( $t_{1/2} = 3.7$  d) and <sup>223</sup>Ra ( $t_{1/2} = 11.4$  d) and the ingrowth of <sup>222</sup>Rn ( $t_{1/2} = 3.8$  d) and <sup>225</sup>Ac ( $t_{1/2} = 10.0$  d). However, prior to counting the disc is stored under counting conditions for at least 1 hour to ensure that <sup>214</sup>Po and <sup>211</sup>Bi are in equilibrium with their parents <sup>222</sup>Rn and <sup>219</sup>Rn respectively.

The <sup>226</sup>Ra activity is measured directly from its peaks at 4.60 and 4.78 MeV. Determination of the activities of <sup>223</sup>Ra and <sup>224</sup>Ra is more complicated; discussion of the procedures involved is deferred to the next section.

The chemical recovery of <sup>225</sup>Ra is determined from the <sup>217</sup>At peak (7.07 MeV). <sup>225</sup>Ra ( $t_{1/2} = 14.8$  d) is a beta-emitter and decays to <sup>225</sup>Ac, which in turn decays to a series of short-lived alpha-emitting daughters, of which only <sup>217</sup>At is conveniently measured (fig 2b). The <sup>225</sup>Ac activity reaches a maximum after 17 days; however, if the activity of the added <sup>225</sup>Ra is high enough, counting can begin any time after deposition.

If a measure of <sup>228</sup>Ra is required, the disc should be stored for at least six months and re-counted (fig 2c). A measure of the <sup>228</sup>Th ingrowth is obtained by analysis of the <sup>224</sup>Ra peak (5.68 MeV, 95%). Flaming of the disc to volatilise <sup>222</sup>Rn is not recommended, as the spectral resolution may be seriously degraded. If the <sup>226</sup>Ra/<sup>228</sup>Ra ratio is high (eg >20), the <sup>224</sup>Ra peak may be difficult to completely resolve from the surrounding <sup>222</sup>Rn and <sup>218</sup>Po peaks. In this case the deposit can be transferred from the disc, and a <sup>228</sup>Th determination carried out (Bojanowski et al 1983).

## Calculation of <sup>225</sup>Ra recovery

If  $A_0$  is the activity of <sup>225</sup>Ra at the time,  $t_0$ , of separation from <sup>229</sup>Th, its activity,

$$A_1 = A_0 \exp\{-\lambda_1(t_1 - t_0)\}$$

where  $\lambda_1$  is the decay probability of <sup>225</sup>Ra. The subsequent activity of <sup>225</sup>Ac at any time,  $A(t)$ , is then given by:

$$A(t) = \frac{\lambda_2 A_1 [\exp\{-\lambda_1(t - t_1)\} - \exp\{-\lambda_2(t - t_1)\}]}{(\lambda_2 - \lambda_1)}$$

where  $\lambda_2$  is the decay probability of <sup>225</sup>Ac.

Integrating over the counting period from  $t_2$  to  $t_3$  gives

$$A(t_2, t_3) = A_1 \frac{\lambda_2}{(\lambda_2 - \lambda_1)(t_3 - t_2)} \left\{ \frac{1}{\lambda_1} [\exp(\lambda_1(t_2 - t_1)) - \exp(-\lambda_1(t_3 - t_1))] - \frac{1}{\lambda_2} [\exp(-\lambda_2(t_2 - t_1)) - \exp(-\lambda_2(t_3 - t_1))] \right\}$$

Hence the recovery of  $^{225}\text{Ra}$  is  $A_m/A(t_2, t_3)$  where  $A_m$  is the measured activity of  $^{217}\text{At}$ .

$$A(t) = \lambda_2 A_1 \frac{\exp\{-\lambda_1(t - t_1)\} - \exp\{-\lambda_2(t - t_1)\}}{(\lambda_2 - \lambda_1)}$$

$$A(t_2, t_3) = A_1 \frac{\lambda_2}{(\lambda_2 - \lambda_1)(t_3 - t_2)} \left\{ \frac{\exp\{-\lambda_1(t_2 - t_1)\} - \exp\{-\lambda_1(t_3 - t_1)\}}{\lambda_1} - \frac{\exp\{-\lambda_2(t_2 - t_1)\} - \exp\{-\lambda_2(t_3 - t_1)\}}{\lambda_2} \right\}$$

## Discussion

### Tracer

If  $^{226}\text{Ra}$  only is to be measured, the quantity of added  $^{225}\text{Ra}$  will depend on the statistical error required, remembering that  $^{225}\text{Ac}$  will grow in to a maximum of only ~44% of the initial  $^{225}\text{Ra}$  spike. If  $^{223}\text{Ra}$  and  $^{224}\text{Ra}$  are to be determined, the  $^{225}\text{Ra}$  spike should be limited, as  $^{225}\text{Ac}$  will slowly grow into the  $^{223}\text{Ra}$  and  $^{224}\text{Ra}$  energy region, and must be stripped from this area before they can be determined (see discussion on  $^{223}\text{Ra}$  and  $^{224}\text{Ra}$  determination below).

As the  $^{225}\text{Ra}$  tracer is added as a daughter product in equilibrium with its parent  $^{229}\text{Th}$ , the thorium/radium separation is required to be quantitative, and the time of separation ( $t_0$ ) known. The complete removal of  $^{225}\text{Ac}$  is also essential, otherwise the fraction remaining on the cation exchange column will be eluted and electrodeposited along with  $^{225}\text{Ra}$ . This will result in an erroneously high recovery figure, the magnitude of which will depend on how soon after deposition the disc is counted. Ingrowth of  $^{225}\text{Ac}$  commences immediately the cation exchange column is converted to the acid form by the HCl wash, and is eluted with 6 M  $\text{HNO}_3$  along with radium. Electrodeposition efficiency is > 90% for both radium and actinium; nevertheless it should be performed without delay (ie on the same day) to minimise the effect of any differences in deposition efficiencies between them.

### Removal of interfering elements

In order to obtain maximum resolution of the alpha-particle spectrum, a very thin source is required. The final radium solution for electrodeposition should therefore be of a high purity, having minimal concentrations of other metal ions. Consequently, the separation procedure must not only remove interfering alpha-emitters, but should chemically isolate radium from alkaline earths and other major metal ions.

Radium, thorium and actinium are coprecipitated from the sample matrix with lead sulphate. Uranium remains in solution. The sulphate ion is then removed by passage through an anion exchange resin. Thorium, lead (Schönfeld et al 1958) and actinium form anionic complexes with EDTA, and are also adsorbed. Radium passes through the anion exchange column in the eluate. Any remaining lead (Khopkar & De 1960), thorium, actinium, polonium or uranium in the eluate is eluted from the following cation exchange column in the ammonium acetate wash. The alkaline earths (calcium, strontium, barium) are eluted sequentially in the 1.5 M ammonium acetate and 2.5 M HCl washes. The decontamination factor for thorium, actinium, polonium, uranium and lead is > 10, and is > 50 for barium.



## Ba-Ra separation

Barium is chemically very similar to radium, and will accompany radium in the lead sulphate lattice during precipitation. Unless removed prior to electrodeposition, it will cause incomplete radium plating, and a poorly resolved alpha-particle spectrum.

Gleason (1979) used DCYTA at pH 8.5 to separate barium and radium. However, the use of complexing agents to obtain separation on a cation exchange column often results in residual traces of the complexing agent contaminating the final radium fraction, adversely affecting electrodeposition. For this reason, 18 column volumes of 2.5 M HCl have been used to wash the ammonium acetate and traces of EDTA from the column prior to the elution of radium.

Both barium and radium are strongly adsorbed in a narrow band at the top of the cation exchange column from 0.025 M EDTA solution at pH 4.5, and are separated by elution with 1.5 M ammonium acetate and 2.5 M HCl. The distribution coefficient for barium is approximately equal in the latter two solutions. Barium-radium separation with HCl, as described in step 4, gave a final radium fraction virtually free from visual residue for most of the groundwater samples analysed. The barium decontamination factor was  $> 50$  ( $> 98\%$  removal of barium). Approximately 3-5% of the radium is sacrificed in the 2.5 M HCl wash. The barium concentrations of the groundwater samples analysed were in the range 50–1000  $\mu\text{g/L}$ . For samples where the barium content was high, the spectral resolution of the source was observed to deteriorate slightly to 50–55 keV FWHM. However, this resolution was still good enough to allow the accurate determination of  $^{223}\text{Ra}$  and  $^{224}\text{Ra}$ .

## Determination of $^{223}\text{Ra}$ and $^{224}\text{Ra}$

Determination of the activities of  $^{223}\text{Ra}$  and  $^{224}\text{Ra}$  is not straight forward, because their direct decay lines overlap in the alpha-particle spectrum. Although their activities can be determined from the observed activities of their daughter products, the analysis procedure must take into account the finite and variable loss of their immediate daughters ( $^{219}\text{Rn}$  and  $^{220}\text{Rn}$  respectively) by emanation from the electrodeposited sample.

Analysis of  $^{223}\text{Ra}$  and  $^{224}\text{Ra}$  on a layer of  $\text{Ba}(\text{Ra})\text{SO}_4$  (Sedlet 1966), has relied on the fact that losses of  $^{219}\text{Rn}$  and  $^{220}\text{Rn}$  through diffusion are minimal due to the thickness of the source. However the spectral peak resolution is poor, and analysis of the daughters as a quantitative measure of the parent radium isotope is difficult due to overlapping of peaks. The use of a limited mass of  $\text{BaSO}_4$  (Sill 1987), yields an improved spectrum, but losses of both  $^{220}\text{Rn}$  and  $^{219}\text{Rn}$  occur from the source, and equilibrium with the parent radium isotope cannot be assumed. In deriving  $^{223}\text{Ra}$  and  $^{224}\text{Ra}$  activities, Lim et al (1989) assumed there was no significant difference in the retention characteristics of  $^{220}\text{Rn}$  and  $^{219}\text{Rn}$  in a source containing 20  $\mu\text{g}$  of barium carrier. The procedure developed here involves the following steps:

- establishment of the value of  $\epsilon$ , the ratio of the retention of  $^{220}\text{Rn}$  to that of  $^{219}\text{Rn}$ , by a separate calibration measurement; this need only be carried out once
- measurement of the total activity of  $^{223}\text{Ra}$  plus  $^{224}\text{Ra}$ ,

$$A_{\text{Ra}} = [^{223}\text{Ra}] + [^{224}\text{Ra}]$$

- measurement of the ratio  $[^{224}\text{Ra}]/[^{223}\text{Ra}]$  for the sample being analysed by measurement of the radon activity ratio,  $[^{220}\text{Rn}]/[^{219}\text{Rn}]$ , and correcting for differential radon loss using  $\epsilon$
- calculation of the  $^{223}\text{Ra}$  and  $^{224}\text{Ra}$  activities from the radium activity ratio and the measured value of the total radium activity,  $A_{\text{Ra}}$

These steps are described in the following paragraphs.

The 5.2–5.9 MeV region includes the  $^{223}\text{Ra}$  and  $^{224}\text{Ra}$  activities as well as in-growing  $^{222}\text{Rn}$  (5.49 MeV), and  $^{225}\text{Ac}$  plus 2%  $^{213}\text{Bi}$  (5.5–5.9 MeV) resulting from the decay of  $^{226}\text{Ra}$  and  $^{225}\text{Ra}$  respectively. This ingrowth can be minimised by counting as soon as possible after deposition. As all radon isotopes will be in secular equilibrium with their daughters, the  $^{222}\text{Rn}$  contribution can be stripped from this region by subtraction of the  $^{214}\text{Po}$  activity at 7.69 MeV. Similarly,  $^{225}\text{Ac}$  and  $^{213}\text{Bi}$  can be stripped by measurement of the  $^{217}\text{At}$  activity. The remaining activity in this region,  $A_{\text{Ra}}$ , is due to  $^{223}\text{Ra}$  and  $^{224}\text{Ra}$ . As both  $^{223}\text{Ra}$  and  $^{224}\text{Ra}$  are usually present in significant quantities in groundwaters, their daughter products must be used to derive their activities. Since both isotopes decay to short-lived gaseous radon isotopes, ( $^{219}\text{Rn}$   $t_{1/2} = 4$  s,  $^{220}\text{Rn}$   $t_{1/2} = 56$  s), losses by diffusion would be expected to occur from a thin source.

To obtain a measure of these losses, 7 sources were prepared as described above containing both  $^{223}\text{Ra}$  and  $^{224}\text{Ra}$ . The  $^{223}\text{Ra}$  and  $^{224}\text{Ra}$  solutions used were separately calibrated against a  $^{226}\text{Ra}$  solution, giving a percentage standard error due to counting statistics on the  $^{224}\text{Ra}/^{223}\text{Ra}$  activity ratio of 0.71%. The measured  $^{220}\text{Rn}/^{219}\text{Rn}$  activity ratio was divided by the calculated  $^{224}\text{Ra}/^{223}\text{Ra}$  activity ratio for each source to give the radon retention ratio,  $\epsilon$  (see table 1). As expected, all values of  $\epsilon$  are  $<1$ , indicating proportionally higher losses of the longer-lived  $^{220}\text{Rn}$  from the source compared with that of  $^{219}\text{Rn}$ . For each individual source the value of  $\epsilon$  appears to be independent, within experimental error, of the measured retention of  $^{220}\text{Rn}$  or  $^{219}\text{Rn}$ , even though these retentions vary from 0.57 to 0.77 between sources. A mean value for  $\epsilon$  of 0.957 was obtained with a standard error of 0.006, and this mean value was used in all sample analyses when determining  $^{223}\text{Ra}$  and  $^{224}\text{Ra}$  activities (see below).

As stated above, the calculation of the  $^{224}\text{Ra}/^{223}\text{Ra}$  activity ratio for a particular sample requires the determination of the observed  $^{220}\text{Rn}/^{219}\text{Rn}$  activity ratio. A measure of  $^{219}\text{Rn}$  can be obtained from the well separated peak at 7.39 MeV due to the decay of its daughter,  $^{215}\text{Po}$ . The  $^{220}\text{Rn}$  activity can be calculated by integrating the count rate observed in the energy region 6.15–6.86 MeV. After subtraction of a small contribution due to  $^{221}\text{Fr}$  at 6.24 and 6.34 MeV (which is given by 85% of the  $^{217}\text{At}$  activity at 7.07 MeV), the activity observed in this region is twice the  $(^{220}\text{Rn} + ^{219}\text{Rn})$  activity; that is, the activity arises from the decay of  $^{220}\text{Rn}$ ,  $^{216}\text{Po}$ ,  $^{219}\text{Rn}$  and  $^{211}\text{Bi}$ . The  $^{220}\text{Rn}$  activity is then half the remaining activity after deducting twice the  $^{219}\text{Rn}$  activity.

Correcting for differential radon loss, the  $^{224}\text{Ra}/^{223}\text{Ra}$  activity ratio is given by

$$R_{\text{Ra}} = (1/\epsilon) [^{220}\text{Rn}]/[^{219}\text{Rn}]$$

and the individual  $^{223}\text{Ra}$  and  $^{224}\text{Ra}$  concentrations obtained from

$$[^{223}\text{Ra}] = A_{\text{Ra}}/(R_{\text{Ra}} + 1)$$

and

$$[^{224}\text{Ra}] = A_{\text{Ra}} R_{\text{Ra}}/(R_{\text{Ra}} + 1)$$

It should be noted that although this spectral stripping technique will yield a  $^{223}\text{Ra}$  determination with a high degree of sensitivity, the statistical accuracy of the  $^{224}\text{Ra}$  determination will suffer in the presence of substantial  $^{223}\text{Ra}$  activity. In this case, the sensitivity of the  $^{224}\text{Ra}$  determination can be improved by obtaining an estimate of the  $^{220}\text{Rn}$  activity from  $^{212}\text{Po}$  at 8.78 MeV, the activity of which is dependent on ingrowth of its  $^{212}\text{Pb}$  grandparent ( $t_{1/2} = 10.6$  h) and parent  $^{212}\text{Bi}$  ( $t_{1/2} = 61$  m). The  $^{220}\text{Rn}/^{219}\text{Rn}$  activity ratio is then given by

$$[^{212}\text{Po}]/(0.64)[^{215}\text{Po}]$$

However, if there is a delay between electrodeposition and the commencement of counting, the disc should be stored under counting conditions, as the  $^{220}\text{Rn}$  retention, and hence  $^{212}\text{Po}$  ingrowth, are inversely related to air pressure. Table 2 shows that the  $^{220}\text{Rn}$  retention of a source

determined at 10 torr pressure is approximately 30% higher than that at 1 atmosphere.  $^{222}\text{Rn}$  shows similar behaviour.

Contamination of the detector by recoiling  $^{222}\text{Rn}$  atoms from the source will, unless prevented, result in an increased background counting rate in the  $^{223}\text{Ra}$  and  $^{224}\text{Ra}$  energy region. Furthermore,  $^{222}\text{Rn}$  on the detector surface is not necessarily in secular equilibrium with its daughters due to recoil losses. This may lead to a serious under-estimate of the  $^{222}\text{Rn}$  activity to be stripped from the  $^{223}\text{Ra}$  and  $^{224}\text{Ra}$  energy region via measurement of  $^{214}\text{Po}$ . Both of these problems were effectively eliminated in the present work by application of the recoil protection technique described in the section on spectroscopy.

**Table 1**  $^{220}\text{Rn}/^{219}\text{Rn}$  retention ratio ( $\epsilon^*$ ) and  $^{220}\text{Rn}$  retentions for 7 standard sources. Counting errors correspond to 1 standard deviation.

Source	$^{220}\text{Rn}$ retention	Retention ratio $\epsilon^*$
ZS776	$0.569 \pm 0.002$	$0.961 \pm 0.010$
ZS773	$0.623 \pm 0.002$	$0.951 \pm 0.010$
ZS766	$0.635 \pm 0.002$	$0.956 \pm 0.012$
ZS767	$0.656 \pm 0.003$	$0.950 \pm 0.015$
ZS772	$0.692 \pm 0.003$	$0.928 \pm 0.010$
ZS764	$0.698 \pm 0.002$	$0.980 \pm 0.008$
ZS765	$0.771 \pm 0.003$	$0.973 \pm 0.011$
mean = 0.957		
standard deviation = 0.016		
standard error = 0.006		

$$* \epsilon = \frac{(^{220}\text{Rn}/^{224}\text{Ra})}{(^{219}\text{Rn}/^{223}\text{Ra})}. \text{ Errors for } \epsilon \text{ include counting and calibration error.}$$

**Table 2**  $^{220}\text{Rn}$  and  $^{222}\text{Rn}$  retention on the same electrodeposited source

	10 torr	760 torr
$^{220}\text{Rn}^a/^{224}\text{Ra}$	$0.632 \pm 0.014$	$0.488 \pm 0.008$
$^{222}\text{Rn}^b/^{226}\text{Ra}$	$0.412 \pm 0.007$	$0.270 \pm 0.007$

a  $^{220}\text{Rn}$  activity determined from the  $^{212}\text{Po}$  peak after an ingrowth period of 60 hours at the specified pressure.

b  $^{222}\text{Rn}$  activity determined after an ingrowth period of 20 days at the specified pressure.

## Intercomparison of results

Results of analyses of three borewater samples taken in the vicinity of the Ranger Uranium Mine tailings dam in November 1988 are presented in table 3. The results obtained using the methods described above are compared with those obtained by the gamma spectrometric determination of a  $\text{MnO}_2/\text{Fe}(\text{OH})_3$  precipitate used to scavenge radium from the borewater. The  $^{224}\text{Ra}$  concentrations were calculated to the time of sample collection, after correcting for support from  $^{228}\text{Th}$ . As the  $^{228}\text{Th}/^{224}\text{Ra}$  activity ratio was  $<0.01$  for most of the groundwater samples analysed, this correction was usually small. Agreement between the two independent techniques for  $^{226}\text{Ra}$ ,  $^{228}\text{Ra}$  and  $^{224}\text{Ra}$  is satisfactory.  $^{223}\text{Ra}$  was not determined by gamma spectrometry.

**Table 3** Comparison of radium isotope concentrations (mBq/L) in groundwaters obtained by alpha-particle and gamma spectrometry. Counting errors quoted correspond to 1 standard deviation.

Bore	<sup>226</sup> Ra		<sup>224</sup> Ra		<sup>228</sup> Ra	
	alpha	gamma	alpha	gamma	alpha	gamma
OB11A	136 ± 6	134 ± 3	58 ± 3	72 ± 11	50 ± 4	53 ± 3
OB13A	68 ± 2	64 ± 2	129 ± 6	145 ± 11	97 ± 4	85 ± 4
OB16	81 ± 3	79 ± 3	250 ± 13	247 ± 28	126 ± 9	125 ± 4

## Summary

The method described in this paper has been developed to enable the preparation of a high resolution source for the determination of all radium isotopes in groundwaters, while attempting to minimise the number of chemical operations and operator time. The use of a <sup>225</sup>Ra tracer enables an accurate measure of the chemical yield. With slight modifications, this method has been successfully applied to a wide range of environmental samples (Hancock & Martin, 1991), and can be incorporated into the radiochemical determination of other naturally occurring radionuclides (<sup>210</sup>Po, uranium, thorium, <sup>227</sup>Ac) on the same sample (Martin & Hancock 1994). The high resolution spectrum has enabled an accurate determination of <sup>224</sup>Ra and <sup>223</sup>Ra via measurement of their daughter products, and <sup>228</sup>Ra after a suitable in-growth period for <sup>228</sup>Th.

## Radium isotopes as seepage indicators in the vicinity of a uranium tailings dam

P Martin and RA Akber

---

### Abstract

Monitoring of bores near the Ranger Uranium Mine tailings dam has revealed deterioration of water quality in several bores since 1983. In a group of bores to the north of the dam, increases have been observed of approximately 100 times for sulphate concentrations and 2 times for  $^{226}\text{Ra}$  activity concentrations.

Measurements of all four naturally-occurring radium isotopes have been used in an investigation of the mechanism responsible for radium concentration increases.  $^{228}\text{Ra}/^{226}\text{Ra}$  ratios have not decreased in affected bores, indicating that the origin of the radium is from the vicinity of the bore rather than being transported directly from the tailings. Increasing borewater salinities are the most probable cause of the  $^{226}\text{Ra}$  increases.

$^{223}\text{Ra}/^{226}\text{Ra}$  and  $^{224}\text{Ra}/^{228}\text{Ra}$  ratios are generally higher in affected bores, and exhibit correlation with sulphate concentrations. These results suggest that the mechanism of radium concentration increases is a complex one, with at least two separate processes involved.

---

### Introduction

The Ranger uranium mine and mill complex is located approximately 260 km east of Darwin in the Northern Territory of Australia (fig 1). The climate is tropical monsoonal, with contrasting Wet (December–March) and Dry (April–November) seasons. Average annual rainfall is about 1550 mm and the annual evaporation is about 1950 mm.

Mining uses a spiral road open-cut pit of about 52 ha surface area. Excavation of the pit commenced in August 1980, with commercial operation of the mill commencing in August 1981. Environmental constraints placed on operations at Ranger have resulted in the establishment of a Restricted Release Zone (RRZ) from which water may not be exported without the approval of the supervising authorities. The RRZ includes the pit, ore stockpiles, mill area, retention ponds 2 and 3 and the tailings dam (fig 2). Operation of Ranger's water management system has been described in detail by Ranger Uranium Mines (1983).

Covering approximately 110 ha of land, the tailings dam is the largest water management structure within the RRZ. Subaqueous tailings deposition was practiced until 1987, but since then sub-aerial deposition methods have been used in order to achieve a greater tailings density.

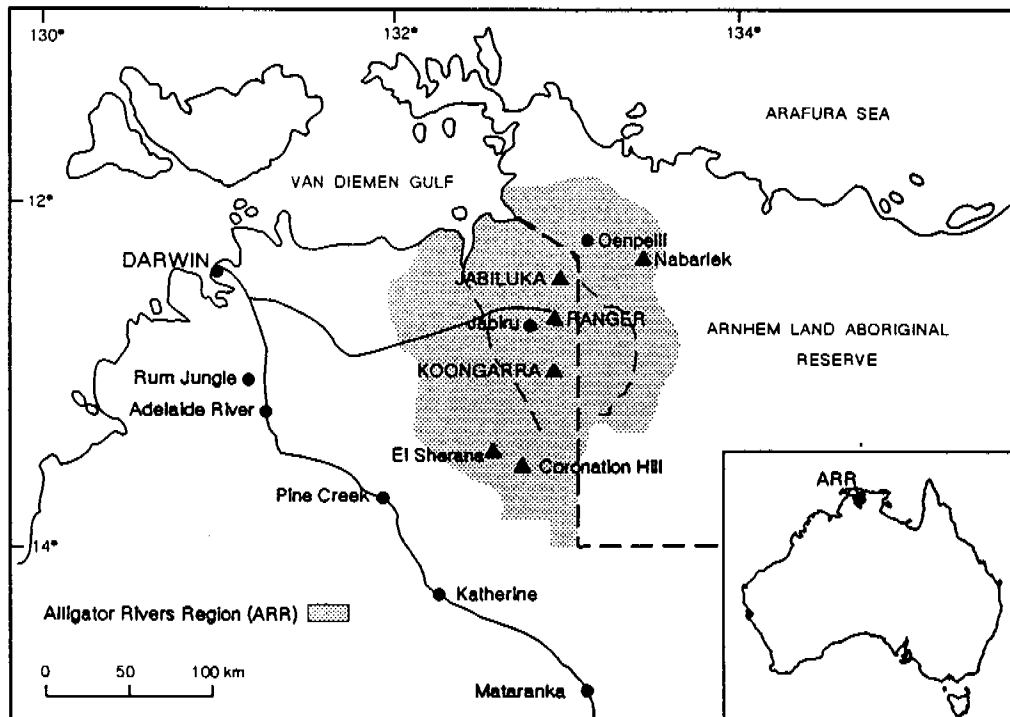


Figure 1 Location of the Ranger uranium mine

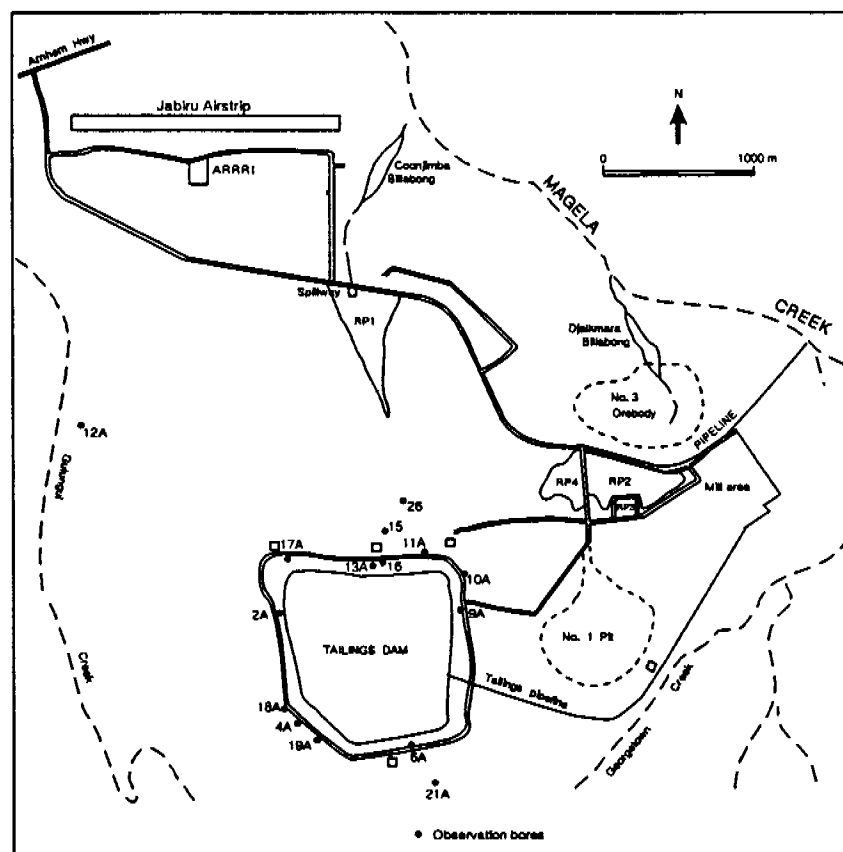


Figure 2 Ranger bore location plan

One of the potential pathways for escape of both radioactive and chemical pollutants from the RRZ is that of groundwater seepage. This pathway concerns both the operational and post-operational rehabilitation phases of the mine; in particular, seepage will need to be considered in any decision on the relative merits of above-ground or pit disposal of tailings in the final rehabilitation of the site.

## Borewater quality and $^{226}\text{Ra}$ concentration changes

Routine monitoring measurements by Ranger have shown deterioration in water quality in several observation bores. Table 1 lists results obtained in 1989 for sulphate and  $^{226}\text{Ra}$  concentrations for a number of bores near the tailings dam. Ratios of these results to those obtained in 1983/84 illustrate the changes which have occurred since the beginning of operations. Sulphate is a particularly sensitive indicator of seepage as its concentration in the tailings water is high (approximately 20,000 mg/L in 1989) due to the use of sulphuric acid as a leachate during processing of the ore.

A group of bores to the north of the dam (OB11A, 13A, 15, 16 and, to a lesser extent, 26; see fig 2) show similar trends in increasing sulphate (approx. 100x) and  $^{226}\text{Ra}$  (approx. 2x).

**Table 1** Sulphate and  $^{226}\text{Ra}$  for a number of Ranger bores

Bore	Sulphate (mg/L) May 1989	Sulphate ratio 1989/1983	$^{226}\text{Ra}$ (mBq/L) 1989	$^{226}\text{Ra}$ ratio 1989/1984
OB11A	790	170	160	3.6
OB16	750	58	100	2.6
OB13A	490	102	80	1.7
OB15	230	56	70	1.4
OB26	* 49	98	390	0.9
OB10A	17	24	93	0.9
OB9A	17	5	66	1.4
OB6A	48	19	360	1.3
OB4A	0.6	8	115	1.3
OB2A	0.4	0.3	42	1.2 **
OB12A	1.8	0.7	58	1.2
OB17A	2.4	0.1	120	0.9
OB18A	* 0.2	0.03	69	1.0
OB19A	<0.2	<0.01	200	1.0
OB21A	<0.2	<0.5	135	0.7

Sulphate data from Ranger Uranium Mines (RUM) environmental monitoring reports; method of analysis was HPLC.  $^{226}\text{Ra}$  activity concentrations used are the means of all measurements available from RUM and OSS data for the respective year. All measurements were performed on an unfiltered ('total') sample.

\* Sulphate concentrations for OB26 and OB18A are for May 1988; sulphate ratios for these bores are for 1988/1983.

\*\*  $^{226}\text{Ra}$  ratio for OB2A is for 1989/1983.

Bores OB10A and 9A have shown increasing sulphate concentrations since 1986. These bores lie between the dam and the pit, and changes in hydrological conditions as the dam is raised and the pit deepened may be an influence on their behaviour. Recent sulphate increases in OB4A near the south-west wall of the dam may indicate seepage in the direction of Gulungul Creek. Increasing sulphate concentrations have also been observed in OB6A, to the south of the dam, since 1983.

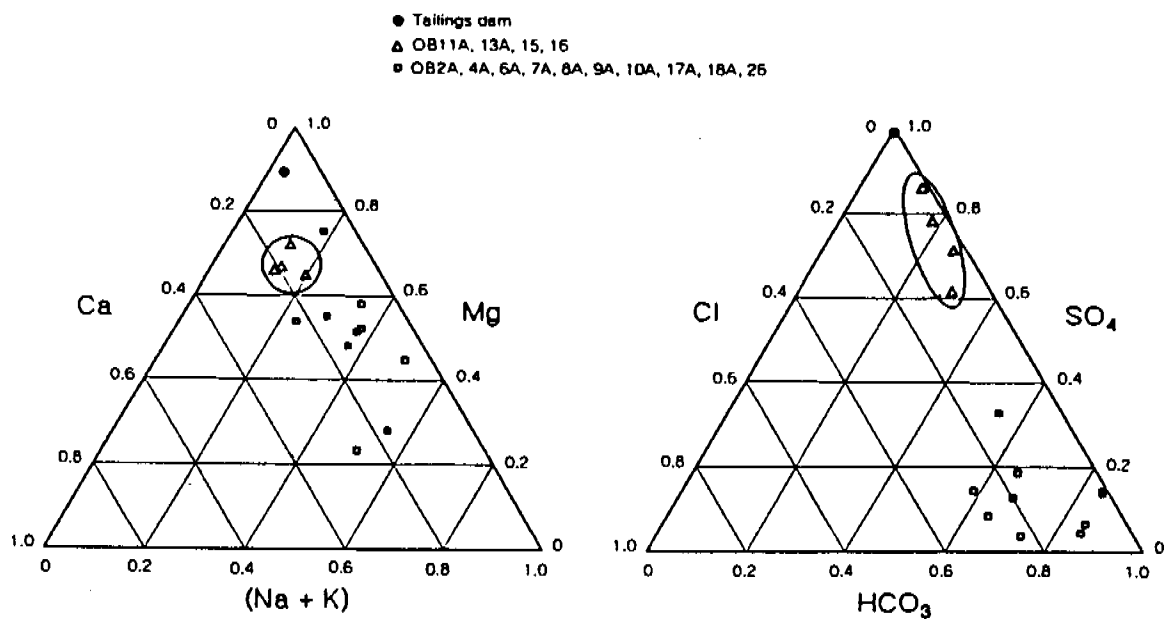


**Figure 3** Cation and anion ternary diagrams for boreholes in the vicinity of the Ranger tailings dam

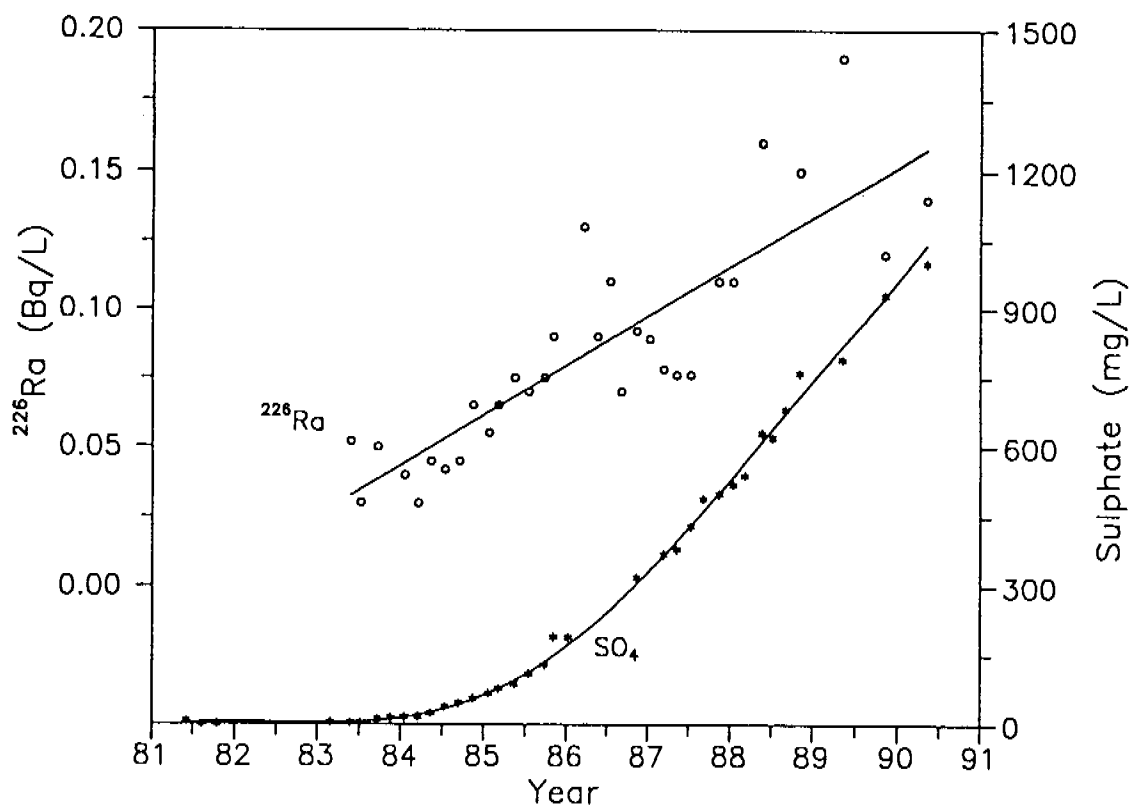


**Figure 4** Bore OB11A <sup>226</sup>Ra and sulphate concentrations



The remaining bores listed in table 1 have shown decreasing sulphate concentrations since 1983. With the exception of OB18A, these decreases occurred entirely over the period 1983–1985, with stable concentrations observed since that time.

Figure 3 shows the relative equivalent concentrations of major cations and anions for tailings dam water and a number of bores measured in May 1989. The bores OB11A, 13A, 15 and 16 form a well-defined group on both ternary diagrams. Sulphate is the dominant anion for these four bores, while bicarbonate dominates for the other bores. This reflects the influence of the tailings dam, for which sulphate constitutes virtually 100% of total anion equivalence. The cation ternary diagram also shows the influence of the tailings dam on these four bores, with magnesium dominating at the expense of (Na + K).

## Radium isotope ratio measurements

Figure 4 shows the variation of  $^{226}\text{Ra}$  and sulphate concentrations with time for one of the affected bores, OB11A, located approximately 100 m from the tailings dam.

The  $^{226}\text{Ra}$  and sulphate concentrations in tailings dam water were approximately 20,000 mBq/L and 20,000 mg/L respectively in 1989. Comparison of the increases in  $^{226}\text{Ra}$  and sulphate concentrations in OB11A between 1983 and 1989 (fig 4) indicates that the seepage velocity for  $^{226}\text{Ra}$  is about 1/10th that of sulphate. This result is somewhat surprising since a substantially larger attenuation would be expected for a reactive element such as radium in comparison with the conservative sulphate ion. These calculations assume, however, that the  $^{226}\text{Ra}$  increases are entirely due to direct transport from the tailings. In order to test whether this assumption is correct, a program of analysis of selected bores for radium isotope ratios was undertaken.

## Experimental

Sampling was timed to coincide with the routine bi-monthly groundwater sampling program of Ranger. Samples were subdivided into a 20 litre subsample in a PVC container for analysis by gamma-ray spectrometry and a 5 litre subsample in a polypropylene container for analysis by alpha-particle spectrometry. Containers and lids were washed with 2%  $\text{HNO}_3$  and rinsed with demineralised water before use, and rinsed three times with bore water immediately before collecting the sample.

For most bores, samples were collected after first pumping the bore for 20 minutes at a flow rate of approximately 5 litres per minute. This was varied only for those bores which were known to be incapable of supplying enough water for a full 20 minutes pumping. On returning to the laboratory, the sample was filtered through a 0.45  $\mu\text{m}$  membrane filter (Millipore HAWP14250).

Gamma-ray spectrometry was used for  $^{226}\text{Ra}$  and  $^{228}\text{Ra}$  measurements. Radionuclides (including radium) were co-precipitated in the 20 litre container with manganese dioxide, followed by a second precipitation using ferric hydroxide. After separation of precipitate from supernatant, the precipitate and filter were ashed, then cast in a mould using a polyester resin before counting on a germanium gamma-ray spectrometer. Casting and analysis techniques have been described in detail in Murray et al (1987).

Alpha-particle spectrometry was used for  $^{223}\text{Ra}$ ,  $^{224}\text{Ra}$ ,  $^{226}\text{Ra}$ ,  $^{228}\text{Ra}$  and  $^{227}\text{Ac}$  determinations. Details of analysis techniques used are described in detail in Hancock & Martin (this publication), and Hancock et al (this publication).

## Results

In May 1985 a number of samples of Ranger observation borewaters were analysed using gamma-ray spectrometry, including samples from three of the affected bores to the north of the dam, OB11A, 13A and 16. Results for the ratio  $^{228}\text{Ra}/^{226}\text{Ra}$  are presented in table 2 for these samples and corresponding samples collected in May 1989.

**Table 2** Variation of  $^{228}\text{Ra}/^{226}\text{Ra}$  ratio with time in 3 affected bores. Errors given represent one standard deviation due to counting statistics.

Bore	Sulphate ratio 1989/1983	$^{228}\text{Ra}/^{226}\text{Ra}$ May 1985	$^{228}\text{Ra}/^{226}\text{Ra}$ May 1989	$\Delta_{\text{Ra}}$ (%)
OB11A	170	$0.20 \pm .02$	$0.38 \pm .02$	$90 \pm 21$
OB13A	102	$1.26 \pm .05$	$1.65 \pm .07$	$31 \pm 8$
OB16	58	$1.71 \pm .06$	$1.45 \pm .06$	$-15 \pm 5$

The final column of table 2 lists values for  $\Delta_{\text{Ra}}$ , the percentage change in the  $^{228}\text{Ra}/^{226}\text{Ra}$  isotopic ratio, defined here as:

$$\Delta_{\text{Ra}} = \{(\text{IR}_{89} - \text{IR}_{85})/\text{IR}_{85}\} \times 100$$

where  $\text{IR}_{85}$  = the  $^{228}\text{Ra}/^{226}\text{Ra}$  isotopic ratio in 1985

$\text{IR}_{89}$  = the  $^{228}\text{Ra}/^{226}\text{Ra}$  isotopic ratio in 1989

The  $^{228}\text{Ra}/^{226}\text{Ra}$  activity ratio in tailings dam water is approximately 0.01. If the tailings dam were the source of  $^{226}\text{Ra}$  increase in these borewaters, a decrease in  $^{228}\text{Ra}/^{226}\text{Ra}$  ratios would be expected to occur, and  $\Delta_{\text{Ra}}$  would be expected to be negative. OB11A and OB13A have values of  $\Delta_{\text{Ra}}$  which are positive, implying that there is little direct contribution from the tailings dam to the  $^{226}\text{Ra}$  concentration increases in these bores. For OB16  $\Delta_{\text{Ra}}$  is negative, though small.

Although the  $^{228}\text{Ra}/^{226}\text{Ra}$  ratio is useful in studying changes in a bore over time, local variations in the  $^{232}\text{Th}/^{238}\text{U}$  ratio in the source rocks complicate its use for comparisons between bores. This problem may be avoided by use of the ratios  $^{223}\text{Ra}/^{226}\text{Ra}$  and  $^{224}\text{Ra}/^{228}\text{Ra}$ .  $^{223}\text{Ra}$  and  $^{226}\text{Ra}$  are members of the  $^{235}\text{U}$  and  $^{238}\text{U}$  decay series, respectively. The activity ratio of these two uranium isotopes in nature is normally 0.046.  $^{224}\text{Ra}$  and  $^{228}\text{Ra}$  are both members of the  $^{232}\text{Th}$  decay series, and their activities should be equal for a system at secular equilibrium.

$^{223}\text{Ra}$  and  $^{224}\text{Ra}$  have short half-lives ( $t_{1/2} = 11$  days and 3.8 days respectively), and would not be expected to be transported long distances in groundwater. Australian Groundwater Consultants (1988) estimate seepage velocities for  $\text{SO}_4$  into the bores to the north of the tailings dam in the range 0.07 to 0.2 m/day, and seepage velocities for radium would not be expected to be greater than those for sulphate. Hence if the radium increase in these bores were caused by direct transport from the dam, the ratios  $^{223}\text{Ra}/^{226}\text{Ra}$  and  $^{224}\text{Ra}/^{228}\text{Ra}$  would be expected to be much lower than their normal equilibrium values at the sampling point due to decay of  $^{223}\text{Ra}$  and  $^{224}\text{Ra}$  during transport.

Table 3 lists average 1988–89 values for these ratios.  $^{223}\text{Ra}/^{226}\text{Ra}$  is significantly above the expected ratio of 0.046 for the four bores with high ( $> 50$  mg/L) sulphate concentrations. There is a similar situation with the  $^{224}\text{Ra}/^{228}\text{Ra}$  ratio, with the ratio being in the range 0.9 to 1.7 for these four bores, and 0.6 to 1.1 for the other bores listed. These findings support the conclusion that radium is originating from the soils in the vicinity of the bores.

**Table 3** Radium isotope ratios for a number of Ranger bores (1988–90)

Bore	Sulphate (mg/L) May 1989	$^{228}\text{Ra}/^{226}\text{Ra}$		$^{223}\text{Ra}/^{226}\text{Ra}$		$^{224}\text{Ra}/^{228}\text{Ra}$		No. samples**	
								$n_8$	$n_{3,4}$
OB11A	790	0.37	± .04	0.07	± .01	1.20	± .07	6	5
OB16	750	1.6	± .2	0.24	± .04	1.7	± .2	5	4
OB13A	490	1.3	± .2	0.18	± .03	1.4	± .1	5	5
OB15	230	2.5	± .6	0.11	± .03	0.9	± .2	4	4
OB26	* 49	0.12	± .01	0.07	± .01	0.9	± .2	4	4
OB10A	17	0.14	± .04	0.024	± (.005)	1.0	± (.2)	2	1
OB9A	17	0.28	± .05	0.05	± .03	0.8	± .4	3	2
OB6A	48	0.18	± .02	0.04	± .01	1.1	± .3	6	4
OB4A	0.6	0.52	± .04	0.036	± .004	0.60	± .01	3	2
OB2A	0.4	1.0	± .5	0.03	± (.01)	0.77	± (.05)	2	1
OB17A	2.4	1.3	± .8	0.03	± .01	0.8	± .2	4	3
OB18A	* 0.2	1.5	± .2	0.047	± .004	0.65	± .06	3	3

\* Sulphate concentrations for OB26 and OB18A are for May 1988.

\*\*  $n_8$  is no. samples analysed for  $^{228}\text{Ra}/^{226}\text{Ra}$  ratio.

$n_{3,4}$  is no. samples analysed for  $^{223}\text{Ra}/^{226}\text{Ra}$  and  $^{224}\text{Ra}/^{228}\text{Ra}$  ratios.

Figures for radium ratios are the mean and standard deviation for all samples analysed between 1988 and 1990. Figures in parentheses represent one standard deviation due to counting statistics where only one sample has been analysed.

## Discussion

The results presented above show that increases in the activity concentrations of all four radium isotopes have occurred in bores affected by seepage. They also indicate that these increases are due, not to direct transport of radium from the tailings dam, but to local soil/solute interactions in the seepage plume. An understanding of the mechanism responsible for the change in radium concentrations observed is necessary before reliable predictions can be made of the long-term exposure of humans resulting from seepage.

Dickson (1985) has studied radium isotopes in borewaters and saline seepages in Western Australia. He found  $^{223}\text{Ra}/^{226}\text{Ra}$  ratios in the range 0.14 to 0.62 for these waters. Chloride ion was in the range 6900 to 57000 mg/L, with sulphate in the range 390 to 5800 mg/L. High  $^{223}\text{Ra}/^{226}\text{Ra}$  ratios were generally associated with high chloride and sulphate concentrations.

Chloride concentrations in the Ranger borewaters are low, being in the range 1 to 30 mg/L for the bores discussed here. Total dissolved ion concentrations have, however, increased substantially in those bores affected by seepage, primarily due to increases in Mg, Ca and  $\text{SO}_4$  concentrations. Figure 5 shows  $^{223}\text{Ra}/^{226}\text{Ra}$  plotted against sulphate concentration for all borewater samples from the Ranger site for which both variables are available. There is a general trend to higher ratios for those bores with higher sulphate concentrations, consistent with the results obtained by Dickson. He postulated that soluble single and double sulphate salts of actinium may be formed, resulting in support of  $^{223}\text{Ra}$  in the water and hence the high ratios. His measurements of the Western Australian waters indicated that there was indeed some support for  $^{223}\text{Ra}$  in the water, with most  $^{227}\text{Ac}/^{223}\text{Ra}$  ratios in the range 0.25 to 0.8.

In order to test whether  $^{223}\text{Ra}$  was being supported by dissolved  $^{227}\text{Ac}$  in the Ranger borewaters,  $^{227}\text{Ac}$  analyses were performed on a number of samples. Analysis was by alpha-particle spectrometry as described in Hancock et al (this publication). The results obtained are summarised in table 4.

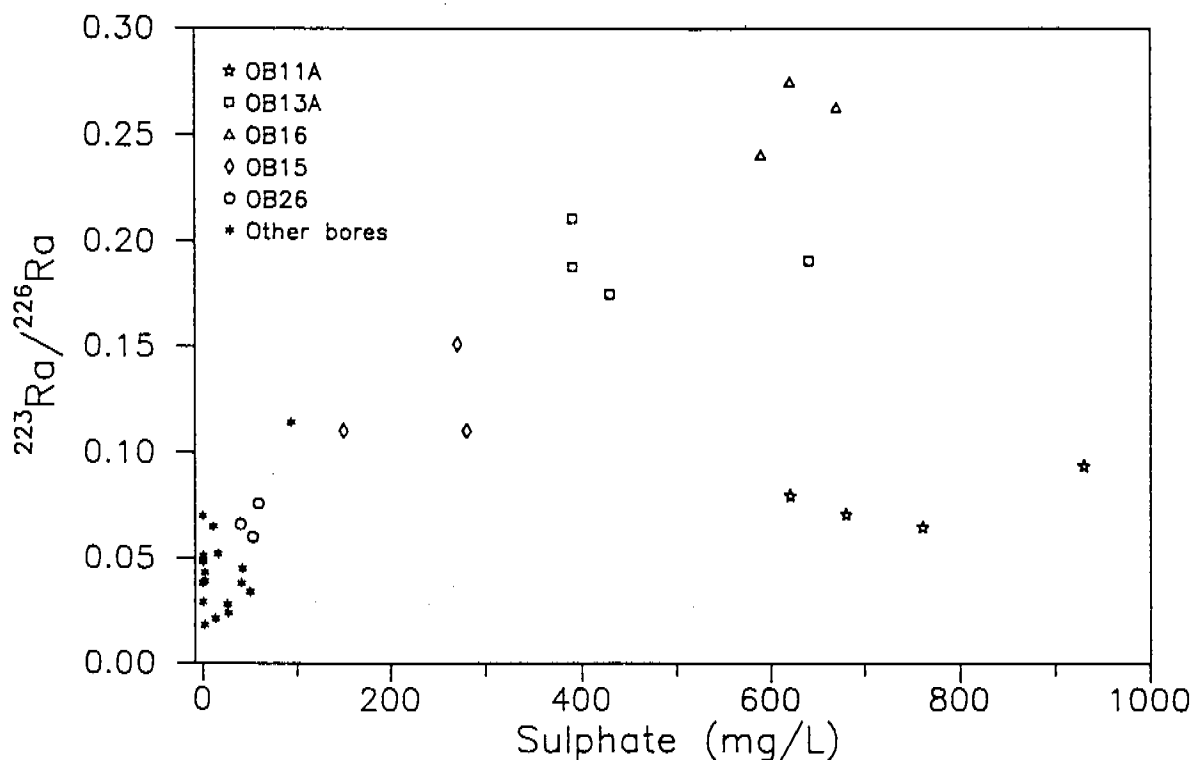


**Figure 5**  $^{223}\text{Ra}/^{226}\text{Ra}$  vs. sulphate for a number of bores near the Ranger tailings dam

The  $^{227}\text{Ac}$  activity concentrations in the high-sulphate bores OB11A, 13A, 15 and 16 are greater than in OB26, 10A and 9A by at least a factor of 2, showing that some actinium mobilisation is occurring. However, in none of the borewaters tested does the  $^{227}\text{Ac}$  activity concentration exceed 7% of that of  $^{223}\text{Ra}$ .

The final column of table 4 shows the ratio of the observed  $^{227}\text{Ac}$  concentration to the  $^{223}\text{Ra}$  concentration which is in excess of the usual value of 0.046 of  $^{226}\text{Ra}$ . This shows that  $^{227}\text{Ac}$  support in the water can account for no more than 3% of the  $^{223}\text{Ra}$  excess in OB13A, 15 and 16, and 25% of the excess in OB11A. In addition,  $^{227}\text{Ac}$  does not decay directly to  $^{223}\text{Ra}$ , but passes through the intermediate thorium isotope  $^{227}\text{Th}$  (half-life 19 days). In the pH range prevailing in these bores (generally pH 6 to 7), most of this  $^{227}\text{Th}$  can be expected to be lost from the water column due to adsorption processes, reducing further the degree of support for  $^{223}\text{Ra}$  in the water.

**Table 4**  $^{227}\text{Ac}$  activity concentrations and  $^{227}\text{Ac}/^{223}\text{Ra}$  activity ratios for a number of Ranger bores. Errors given represent one standard deviation due to counting statistics.

Bore	Sulphate (mg/L) May 1989	$^{227}\text{Ac}$ (mBq/L)	$^{223}\text{Ra}/^{226}\text{Ra}$	$^{227}\text{Ac}/^{223}\text{Ra}$	$^{227}\text{Ac}$ $^{223}\text{Ra}$ excess **
OB11A	790	0.65 ± .07	0.065 ± .005	0.07 ± .01	0.25 ± .07
OB16	750	0.47 ± .07	0.263 ± .019	0.022 ± .004	0.027 ± .005
OB13A	490	0.37 ± .08	0.191 ± .012	0.023 ± .005	0.031 ± .007
OB15	230	0.20 ± .04	0.151 ± .020	0.024 ± .006	0.035 ± .010
OB26	* 49	<0.1	0.058 ± .003	<0.005	
OB10A	17	<0.08	0.024 ± .005	<0.08	
OB9A	17	<0.06	0.064 ± .008	<0.02	

\* Sulphate concentration for OB26 is for May 1988.

\*\*  $^{223}\text{Ra}$  excess is the difference between the observed  $^{223}\text{Ra}$  activity concentration and that expected from the  $^{226}\text{Ra}$  activity concentration using the usual activity ratio of the two decay series of 0.046.

Although fig 5 shows that a relationship exists between sulphate and the  $^{223}\text{Ra}/^{226}\text{Ra}$  ratio in the Ranger bores, it does not establish sulphate as a cause of high ratios, as there are strong correlations for sulphate with a number of other parameters in these waters, particularly conductivity and magnesium and calcium concentrations.

Dickson (1985) performed laboratory experiments in which crushed uraninite–allanite ore samples were leached in NaCl and NaCl + Na<sub>2</sub>SO<sub>4</sub> solutions. In the absence of sulphate ion, increasing the Na ion concentration led to an increase in the activity concentration of all four radium isotopes in solution, while the  $^{223}\text{Ra}/^{226}\text{Ra}$  and  $^{224}\text{Ra}/^{228}\text{Ra}$  ratios remained constant. Increasing sulphate concentration at constant chloride concentration had the effect of increasing these two ratios, even though absolute radium concentrations were initially depressed. This experiment shows that high sulphate concentration is indeed a strong causal factor for high  $^{223}\text{Ra}/^{226}\text{Ra}$  and  $^{224}\text{Ra}/^{228}\text{Ra}$  ratios.

Langmuir and Riese (1985) and Langmuir and Melchior (1985) have studied the trace aqueous and solid solution chemistry of radium and concluded that, since radium concentrations in groundwaters are always too low to reach saturation with respect to a pure radium phase, concentrations will be limited either by adsorption reactions or by solid solution formation. On the basis of the results presented here, we conclude that a combination of both of these processes is affecting radium isotope concentrations in the Ranger borewaters.

The increases in concentrations of major cations observed as a result of seepage can be expected to cause desorption of available radium due to increased competition for adsorption sites. Adsorption–desorption reactions have reaction rates of the order of seconds to hours (Langmuir and Riese, 1985), and equilibrium is likely to be reached in times much shorter than the half-lives of the four radium isotopes. Hence, at equilibrium, radium isotope ratios on such sites will be equal to the ratios in the water. Although subsequent release from such sites may cause increases in radium concentrations in the water, this should not affect isotope ratios.

Formation of a solid solution, on the other hand, would result in the removal of radium from the water. The reverse reaction rate (ie the rate of redissolution of radium from the solid phase) can be expected to be small in comparison with the radioactive decay rates of  $^{223}\text{Ra}$  and  $^{224}\text{Ra}$ , and the  $^{223}\text{Ra}/^{226}\text{Ra}$  and  $^{224}\text{Ra}/^{228}\text{Ra}$  isotope ratios on such a reaction site would be lower than the corresponding ratio in the water due to subsequent decay of the shorter-lived isotope. Assuming that the rate of supply of radium atoms due to parent decay in the source rocks remains constant, the isotope ratios in the total system of water plus adsorption sites plus solid solution must remain constant. Consequently, a decrease in an isotope ratio in the solid solution phase must be accompanied by an increase in the same ratio in the water as a new equilibrium position is approached.

The exact nature of this solid solution phase has yet to be determined. The relationship between the  $^{223}\text{Ra}/^{226}\text{Ra}$  ratio and sulphate concentration seen in fig 5 suggests that it is a sulphate mineral. Note that four points in fig 5, all representing bore OB11A, lie below the trend line for the other bores. Further work may enable us to determine why this bore is behaving differently, and help determine the nature of the solid phase.

---

## Conclusions

A major problem for most studies of borewater radium concentrations to date has been between –bore variation in the large number of relevant physical and chemical parameters. This can result in significant differences in behaviour even between bores which are geographically close and nominally accessing the same aquifer. This is illustrated by the case of bore OB11A which, although located only approximately 300 m from bores OB13A, 15 and 16 and experiencing

similar seepage levels, exhibits markedly different  $^{228}\text{Ra}/^{226}\text{Ra}$  ratios (tables 2 & 3),  $^{227}\text{Ac}/^{223}\text{Ra}$  ratios (table 4) and isotope ratio vs. sulphate behaviour (fig 5).

An advantage of the Ranger case is that we can study changes in bores with time as a relatively small number of parameters change. A baseline database has now been established for uranium and thorium series radionuclides, in particular radium and  $^{227}\text{Ac}$ , for almost all of the bores in the vicinity of the dam. Monitoring of bores such as OB10A, 9A and 4A, which are showing the early effects of seepage, may enable us to confirm the utility of these isotopes as seepage indicators.

$^{226}\text{Ra}$  activity concentrations in the bores to the north of the dam are continuing to increase, and the ultimate equilibrium value cannot as yet be predicted. Radium concentrations can also be expected to increase in any bores exhibiting salinity increases in the future. Any dose rate calculations would need to take into account  $^{228}\text{Ra}$  as well as  $^{226}\text{Ra}$ , as both isotopes are mobilized.

---

## Acknowledgments

Water quality data presented in figures 3 and 4 and sulphate concentration data quoted elsewhere in this paper have been obtained from Ranger Uranium Mine's environmental monitoring reports.

A number of people have helped with sample collection and analysis over the course of this study. We would particularly like to thank Rainer Marten, John Pfitzner and Gary Hancock for their assistance.

## References

- Akber R, Pfitzner J & Johnston A 1991. Public radiation dose due to radon transport from Ranger Uranium Mine. Internal report 24, Supervising Scientist for the Alligator Rivers Region, Canberra. Unpublished paper.
- Anderson RF & Fleer AP 1982. Determination of natural actinides and plutonium in marine particulate material. *Analytical Chemistry* 54, 1142–1147.
- ARRRI 1991. *Alligator Rivers Region Research Institute: Annual research summary 1985–86*. Supervising Scientist for the Alligator Rivers Region, AGPS, Canberra, 47–52.
- Australian Groundwater Consultants Pty Ltd 1988. Groundwater monitoring review and proposed revised monitoring program. Report to Ranger Uranium Mines, August 1988.
- Bojanowski R, Fukai S, Ballestra S & Asari H 1983. Determination of natural radioactive elements in marine environmental materials by ion-exchange and alpha-spectrometry. *Proceedings from the 4th Symposium on the Determination of Radionuclides in Environmental and Biological Materials*, Paper No. 9, Laboratory of the Government Chemist, London.
- Bojanowski R, Holm E, Whitehead NE 1987. Determination of  $^{227}\text{Ac}$  in environmental samples by ion-exchange and alpha spectrometry. *Journal of Radioanalytical and Nuclear Chemistry Articles* 115, 23–37.
- Clark GH 1977. Assessment of the meteorological data and atmospheric dispersion estimates in the Ranger 1 uranium mining impact statement Report AAEC/E407 ISBN 0 642 99772 1 Australian Atomic Energy Commission, Lucas Heights.
- Clark GH, Petersen MCE, Barstch FJK, Pfitzner J & Akber R 1993. The climatology and air pollution meteorology at Jabiru East, Northern Territory 1988 to 1990. Open file record 87, Supervising Scientist for the Alligator Rivers Region, Canberra. Unpublished paper.
- CODE 1987. *Code of practice on radiation protection in the mining and milling of radioactive ores 1987*. AGPS, Canberra.
- Debertin K & Helmer RG 1988. Gamma- and X-ray spectrometry with semiconductor detectors. Elsevier Science Publishers B.V, Amsterdam. 102–103.
- Dickson BL, Meakins RL & Bland CJ 1983. Evaluation of radioactive anomalies using radium isotopes in groundwaters. *Journal of Geochemical Exploration* 19, 195–205.
- Dickson BL 1985. Radium isotopes in saline seepages, south-western Yilgarn, Western Australia. *Geochimica et Cosmochimica Acta* 49, 361–368.
- Gleason G 1979. An improved ion exchange procedure for the separation of barium from radium. *Proceedings of 23rd Conference on Analytical Chemistry in Energy Technology*.
- Hancock GJ & Martin P 1991. Determination of Ra in environmental samples by alpha-particle spectrometry. *International Journal of Applied Radiation and Isotopes* 42, 63–69.
- Hendee WR 1984. Radioactive isotopes in biological research.
- ICRP 1991. *Annual limits on intake of radionuclides by workers based on the 1990 recommendations*, ICRP Publication 61, Pergamon Press, Oxford.
- Khopkar SM & De AK 1960. Cation-exchange behaviour of barium on Dowex 50W-X8. *Analytica Chimica Acta* 23, 441–445.

- Knoll GF 1979. *Radiation detection and measurement*. John Wiley & Sons, New York.
- Koide M & Bruland KW 1975. The electrodeposition and determination of radium by isotopic dilution in sea water and in sediments simultaneously with other natural radionuclides. *Analytica Chimica Acta* 75, 1–19.
- Kvasnicka J 1990. Radon daughters in tropical Northern Australia and the environmental radiological impact of uranium mining. Dept Mines and Energy, Darwin.
- LaBrecque JJ, Dekner R, Hanna AN, Reichel F, Rassoul A & Schelenz R 1987. *Intercomparison study IAEA/SL-2 on the determination of environmental levels of radioactivity in lake sediment*. International Atomic Energy Agency, Vienna, IAEA/RL/142.
- Langmuir D & Melchior D 1985. The geochemistry of Ca, Sr, Ba and Ra sulfates in some deep brines from the Palo Duro Basin, Texas. *Geochimica et Cosmochimica Acta* 49, 2423–2432.
- Langmuir D & Riese AC 1985. The thermodynamic properties of radium. *Geochimica et Cosmochimica Acta* 49, 1593–1601.
- Lederer CM & Shirley VS 1978. *Table of the isotopes*, 7th edn. John Wiley & Sons, New York.
- Lim TP, Dave NK & Cloutier NR 1989. High resolution alpha-particle-spectrometry for radium analysis: The effects of sample thickness and filter pore size. *International Journal of Applied Radiation and Isotopes* 40, 63–71.
- Martin P & Hancock G 1992. *Routine analysis of naturally occurring radionuclides in environmental samples by alpha-particle spectrometry*. Research report 7, Supervising Scientist for the Alligator Rivers Region, AGPS, Canberra.
- Murray AS, Marten R, Johnston A & Martin P 1987. Analysis for naturally occurring radionuclides at environmental concentrations by gamma spectrometry. *Journal of Radioanalytical and Nuclear Chemistry, Articles*, vol 115, no 2, 263–288.
- NATMAP 1986. *Atlas of Australian Resources*. Third series. Volume 4 : Climate. Division of National Mapping, Canberra.
- NCRP 1988. *Measurement of radon and radon daughters in air*. NCRP Report No. 97, National Council on Radiation Protection and Measurements, Bethesda, USA.
- Nozaki Y 1984. Excess  $^{227}\text{Ac}$  in deep ocean water. *Nature* 310, 486–488.
- Pfützner J & Whittlestone S 1991. Automatic environmental radon station: Operators manual. Internal report 25, Supervising Scientist for the Alligator Rivers Region, Canberra. Unpublished paper.
- Ranger Uranium Mines Pty Ltd 1983. Ranger uranium mine water management system. *Water*, 10, 13–18.
- Riley PA 1989. The diurnal variation of the low level jet over the Northern Territory. Bureau of Meteorology, Meteorology Note No. 188. Unpublished paper.
- Schönfeld T, Wald M & Brund M 1958. Radiochemical separations on anion exchange columns with employment of strong complexing agents. *Proceedings of the Second International Conference on the Peaceful Uses of Atomic Energy*, Geneva, 28, 48–54, United Nations.
- Sedlet J 1966. Radon and radium. In *Treatise on analytical chemistry, Part II: Analytical chemistry of the elements*, vol 4, eds IM Kolthoff & PJ Elving. Interscience, New York, 219–366.



- Short SA 1986. Measurement of all radium isotopes at environmental levels on a single electrodeposited source. *Nuclear Instruments and Methods in Physics Research*, B17, 540–544.
- Sill CW & Olson DG 1970. Sources and prevention of recoil contamination of solid-state alpha detectors. *Analytical Chemistry* 42, 1596–1607.
- Sill CW 1987. Determination of radium-226 in ores, nuclear wastes and environmental samples by high-resolution alpha spectrometry. *Nuclear and Chemical Waste Management* 7, 239–256.
- Smith KA & Mercer ER 1970. The determination of  $^{226}\text{Ra}$  and  $^{228}\text{Ra}$  in soils and plants using  $^{225}\text{Ra}$  as a yield tracer. *Journal of Radioanalytical Chemistry* 5, 303–312.
- Strong KP & Levins DM 1982. Effect of moisture content on radon emanation from uranium ore and tailings. *Health Physics* 42, 27–32.
- Talvitie NA 1972. Electrodeposition of actinides for alpha spectrometric determination. *Analytical Chemistry* 44, 280–283.
- Whittlestone S 1985. A high-sensitivity Rn detector incorporating a particle generator. *Health Physics* 49, 847–52.
- Whittlestone S 1992. Radon and radon daughter transport from Ranger uranium mine. Open file record 77, Supervising Scientist for the Alligator Rivers Region, Canberra. Unpublished paper.
- Woods DA 1989. *Concentration of radon and radon daughters during semi-dry tailings deposition by QML at Nabarlek (1985-88)*. Technical memorandum 29, Supervising Scientist for the Alligator Rivers Region, AGPS, Canberra.
- Yamartino RJ 1984. A comparison of several single pass estimators of the standard deviation of wind direction. *Journal of Climate and Applied Meteorology* 23, 1362–1366.

---

Supervising Scientist for the Alligator Rivers Region

## Research publications

Alligator Rivers Region Research Institute Research Report 1983  
Alligator Rivers Region Research Institute Annual Research Summary 1984-85  
Alligator Rivers Region Research Institute Annual Research Summary 1985-86  
Alligator Rivers Region Research Institute Annual Research Summary 1986-87  
Alligator Rivers Region Research Institute Annual Research Summary 1987-88  
Alligator Rivers Region Research Institute Annual Research Summary 1988-89  
Alligator Rivers Region Research Institute Annual Research Summary 1990-91  
Alligator Rivers Region Research Institute Annual Research Summary 1991-92 (in press)

---

## Research reports

- RR1 Marchant R 1982. *The macroinvertebrates of Magela Creek, Northern Territory*. Research report 1, Supervising Scientist for the Alligator Rivers Region, AGPS, Canberra. (46pp)
- RR2 Hart BT & McGregor RJ 1982. *Water quality characteristics of eight billabongs in the Magela Creek catchment*. Research report 2, Supervising Scientist for the Alligator Rivers Region, AGPS, Canberra. (60pp)
- RR3 Thomas DP 1983. *A limnological survey of the Alligator Rivers Region. Volume I Diatoms (Bacillariophyceae) of the Region*. Research report 3 (i), Supervising Scientist for the Alligator Rivers Region, AGPS, Canberra. (160pp)
- Ling HU & Tyler PA 1983. *A limnological survey of the Alligator Rivers Region. Volume II Freshwater algae, exclusive of diatoms*. Research report 3 (ii), Supervising Scientist for the Alligator Rivers Region, AGPS, Canberra. (176pp)
- RR4 Bishop KA, Allen SA, Pollard DA & Cook MG 1986. *Ecological studies on the freshwater fishes of the Alligator Rivers Region, Northern Territory. Volume I Outline of the study, summary, conclusions and recommendations*. Research report 4 (i), Supervising Scientist for the Alligator Rivers Region, AGPS, Canberra. (63pp)
- Bishop KA, Allen SA, Pollard DA & Cook MG 1990. *Ecological studies on the freshwater fishes of the Alligator Rivers Region, Northern Territory. Volume II Synecology*. Research report 4 (ii), Supervising Scientist for the Alligator Rivers Region, AGPS, Canberra. (155pp)
- Bishop KA, Allen SA, Pollard DA & Cook MG (in press). *Ecological studies on the freshwater fishes of the Alligator Rivers Region, Northern Territory. Volume III Autecology*. Research report 4 (iii), Supervising Scientist for the Alligator Rivers Region, AGPS, Canberra.
- RR5 Finlayson CM, Bailey BJ & Cowie ID 1989. *Macrophyte vegetation of the Magela Creek flood plain, Alligator Rivers Region, Northern Territory*. Research report 5, Supervising Scientist for the Alligator Rivers Region, AGPS, Canberra. (41pp)

- RR6 Wasson RJ 1992. *Modern sedimentation and late quaternary evolution of the Magela Creek Plain*. Research report 6, Supervising Scientist for the Alligator Rivers Region, AGPS, Canberra. (349pp)
- RR7 Martin P & Hancock G 1992. *Routine analysis of naturally occurring radionuclides in environmental samples by alpha-particle spectrometry*. Research report 7, Supervising Scientist for the Alligator Rivers Region, AGPS, Canberra. (119pp)
- RR8 Murray AS, Johnston A, Martin P, Hancock G, Marten R & Pfitzner J (in press). *Transport of naturally occurring radionuclides in the surface waters of the Magela Creek and flood plain, northern Australia*. Research report 8, Supervising Scientist for the Alligator Rivers Region, AGPS, Canberra.
- RR9 Woodland DJ & Ward PJ 1992. *Fish communities in sandy pools of Magela Creek, Alligator Rivers Region*. Research report 9, Supervising Scientist for the Alligator Rivers Region, AGPS, Canberra. (88pp)
- RR10 Willett IR, Bond WJ, Akber RA, Lynch DJ & Campbell GD 1993. *The fate of water and solutes following irrigation with retention pond water at Ranger Uranium Mine*. Research report 10, Supervising Scientist for the Alligator Rivers Region, AGPS, Canberra. (132pp)

---

## Technical memoranda

- TM1 Hart BT, Davies SHR & Thomas PA 1981. *Transport of trace metals in the Magela Creek system, Northern Territory: I Concentrations and loads of iron, manganese, cadmium, copper, lead and zinc during flood periods in the 1978-1979 Wet season*. Technical memorandum 1, Supervising Scientist for the Alligator Rivers Region, AGPS, Canberra. (23pp)
- TM2 Davies SHR & Hart BT 1981. *Transport of trace metals in the Magela Creek system, Northern Territory: II Trace metals in the Magela Creek billabongs at the end of the 1978 Dry season*. Technical memorandum 2, Supervising Scientist for the Alligator Rivers Region, AGPS, Canberra. (23pp)
- TM3 Thomas PA, Davies SHR & Hart BT 1981. *Transport of trace metals in the Magela Creek system, Northern Territory: III Billabong sediments*. Technical memorandum 3, Supervising Scientist for the Alligator Rivers Region, AGPS, Canberra. (24pp)
- TM4 Recher HR & Holmes RT 1982. *The foraging behaviour of herons and egrets on the Magela Creek flood plain, Northern Territory*. Technical memorandum 4, Supervising Scientist for the Alligator Rivers Region, AGPS, Canberra. (20pp)
- TM5 Hart BT & McGregor RJ 1982. *Flocculation of retention pond water*. Technical memorandum 5, Supervising Scientist for the Alligator Rivers Region, AGPS, Canberra. (8pp)
- TM6 James CD, Morton SR, Braithwaite RW & Wombey JC 1984. *Dietary pathways through lizards of the Alligator Rivers Region, Northern Territory*. Technical memorandum 6, Supervising Scientist for the Alligator Rivers Region, AGPS, Canberra. (15pp)
- TM7 Hart BT & Davies SHR 1984. *Capacity of waters in the Magela Creek system, Northern Territory, to complex copper and cadmium*. Technical memorandum 7, Supervising Scientist for the Alligator Rivers Region, AGPS, Canberra. (42pp)
- TM8 Baker L & Walden D 1984. *Acute toxicity of copper and zinc to three fish species from the Alligator Rivers Region*. Technical memorandum 8, Supervising Scientist for the Alligator Rivers Region, AGPS, Canberra. (31pp)

- TM9 Thomas PA & Hart BT 1984. *Textural characteristics and heavy metal concentrations in billabong sediments from the Magela Creek system, northern Australia*. Technical memorandum 9, Supervising Scientist for the Alligator Rivers Region, AGPS, Canberra. (39pp)
- TM10 Hart BT & Jones MJ 1984. *Oxidation of manganese (II) in Island Billabong water*. Technical memorandum 10, Supervising Scientist for the Alligator Rivers Region, AGPS, Canberra. (11pp)
- TM11 Hart BT, Jones MJ & Breen P 1984. *In situ experiments to determine the uptake of copper by the aquatic macrophyte *Najas tenuifolia* R. Br.* Technical memorandum 11, Supervising Scientist for the Alligator Rivers Region, AGPS, Canberra. (13pp)
- TM12 Hart BT, Jones MJ & Bek P 1985. *Use of plastic enclosures in determining the effects of heavy metals added to Gulungul Billabong*. Technical memorandum 12, Supervising Scientist for the Alligator Rivers Region, AGPS, Canberra. (25pp)
- TM13 Hart BT, Jones MJ & Bek P 1985. *Fate of heavy metals in the Magela Creek system, northern Australia: I Experiments with plastic enclosures placed in Island Billabong during the 1980 Dry season – heavy metals*. Technical memorandum 13, Supervising Scientist for the Alligator Rivers Region, AGPS, Canberra. (46pp)
- TM14 Hart BT, Jones MJ, Bek P & Kessell J 1985. *Fate of heavy metals in the Magela Creek system, northern Australia: II Experiments with plastic enclosures placed in Island Billabong during the 1980 Dry season – limnology and phytoplankton*. Technical memorandum 14, Supervising Scientist for the Alligator Rivers Region, AGPS, Canberra. (32pp)
- TM15 Smith DI, Young PC & Goldberg RJ 1986. *Use of fluorometric dye tracing to simulate dispersion of discharge from a mine site: A study of the Magela Creek system, March 1978*. Technical memorandum 15, Supervising Scientist for the Alligator Rivers Region, AGPS, Canberra. (51pp)
- TM16 Shine R 1986. *Diets and abundances of aquatic and semi-aquatic reptiles in Alligator Rivers Region*. Technical memorandum 16, Supervising Scientist for the Alligator Rivers Region, AGPS, Canberra. (57pp)
- TM17 Cowie IE & Finlayson CM 1986. *Plants of the Alligator Rivers Region, Northern Territory*. Technical memorandum 17, Supervising Scientist for the Alligator Rivers Region, AGPS, Canberra. (54pp)
- TM18 Julli ME 1986. *The taxonomy and seasonal population dynamics of some Magela Creek flood plain microcrustaceans (*Cladocera* and *Copepoda*)*. Technical memorandum 18, Supervising Scientist for the Alligator Rivers Region, AGPS, Canberra. (80pp)
- TM19 Tyler MJ & Crook GA 1987. *Frogs of the Magela Creek system*. Technical memorandum 19, Supervising Scientist for the Alligator Rivers Region, AGPS, Canberra. (46pp)
- TM20 Johnston A 1987. *Radiation exposure of members of the public resulting from operations of the Ranger Uranium Mine*. Technical memorandum 20, Supervising Scientist for the Alligator Rivers Region, AGPS, Canberra. (22pp)
- TM21 Anttonen T, Noller BN & Woods DA 1988. *Interlaboratory comparison of the measurement of uranium in urine*. Technical memorandum 21, Supervising Scientist for the Alligator Rivers Region, AGPS, Canberra. (24pp)
- TM22 Ivantsoff W, Crowley LELM, Howe E & Semple G 1988. *Biology and early development of eight fish species from the Alligator Rivers Region*. Technical memorandum 22, Supervising Scientist for the Alligator Rivers Region, AGPS, Canberra. (68pp)

- TM23 Cowie ID, Finlayson CM & Bailey BJ 1988. *Alien plants in the Alligator Rivers Region, Northern Territory, Australia*. Technical memorandum 23, Supervising Scientist for the Alligator Rivers Region, AGPS, Canberra. (34pp)
- TM24 leGras CAA & Noller BN 1989. *The determination of zinc in Magela Creek water*. Technical memorandum 24, Supervising Scientist for the Alligator Rivers Region, AGPS, Canberra. (26pp)
- TM25 Allison HE & Simpson RD 1989. *Element concentrations in the freshwater mussel, Velesunio angasi, in the Alligator Rivers Region*. Technical memorandum 25, Supervising Scientist for the Alligator Rivers Region, AGPS, Canberra. (262pp)
- TM26 Vardavas IM & Cannon LM 1989. *A simple computer model for terrestrial and solar radiation transfer*. Technical memorandum 26, Supervising Scientist for the Alligator Rivers Region, AGPS, Canberra. (60pp)
- TM27 Vardavas IM 1992. *Annual rainfall statistics for stations in the Top End of Australia: Normal and log-normal distribution analysis*. Technical memorandum 27, Supervising Scientist for the Alligator Rivers Region, AGPS, Canberra. (34pp)
- TM28 Noller BN, McBride TP, Hunt CW & Hart BT 1989. *A study of the reproducibility of water conditions between small enclosures and a tropical waterbody*. Technical memorandum 28, Supervising Scientist for the Alligator Rivers Region, AGPS, Canberra. (20pp)
- TM29 Woods DA 1989. *Concentration of radon and radon daughters during semi-dry tailings deposition by QML at Nabarlek (1985-88)*. Technical memorandum 29, Supervising Scientist for the Alligator Rivers Region, AGPS, Canberra. (35pp)
- TM30 Carter MW 1990. *The development of a regulatory mechanism for the control of water release from Ranger Uranium Mine*. Technical memorandum 30, Supervising Scientist for the Alligator Rivers Region, AGPS, Canberra. (31pp)
- TM31 Riley SJ & East TJ 1990. *Investigation of the erosional stability of waste rock dumps under simulated rainfall: a proposal*. Technical memorandum 31, Supervising Scientist for the Alligator Rivers Region, AGPS, Canberra. (56pp)
- TM32 Sadler RA 1990. *The terrestrial and semiaquatic reptiles (Lacertilia, Serpentes) of the Magela Creek region, Northern Territory*. Technical memorandum 32, Supervising Scientist for the Alligator Rivers Region, AGPS, Canberra. (86pp)
- TM33 Stockwell DR, Bentley KW & Kerr CB 1991. *In vitro dissolution of uranium mill products by the batch replacement method*. Technical memorandum 33, Supervising Scientist for the Alligator Rivers Region, AGPS, Canberra. (24pp)
- TM34 Chartres CJ, Walker PH, Willett IR, East TJ, Cull RF, Talsma T & Bond WJ 1991. *Soils and hydrology of Ranger Uranium Mine sites in relation to application of retention pond water*. Technical memorandum 34, Supervising Scientist for the Alligator Rivers Region, AGPS, Canberra. (69pp)
- TM35 leGras CAA & Noller BN 1991. *The determination of low concentrations of sodium, potassium, magnesium, calcium and strontium in natural waters by graphite furnace AAS*. Technical memorandum 35, Supervising Scientist for the Alligator Rivers Region, AGPS, Canberra. (18pp)
- TM36 Brennan KG, Noller BN, leGras CAA, Morton SR & Dostine PL 1992. *Heavy metals in waterbirds from the Magela Creek flood plain, Alligator Rivers Region, Northern Territory, Australia*. Technical memorandum 36, Supervising Scientist for the Alligator Rivers Region, AGPS, Canberra. (59pp)

- TM37 Padovan A 1992. *Isolation and culture of five species of freshwater algae from the Alligator Rivers Region, Northern Territory*. Technical memorandum 37, Supervising Scientist for the Alligator Rivers Region, AGPS, Canberra. (30pp)
  
- TM38 Carter MW, Burns P, & Munslow-Davies L 1993. *Radiotoxicity hazard classification: the basis and development of a new list*. Technical memorandum 38, Supervising Scientist for the Alligator Rivers Region, AGPS, Canberra. (23pp)
  
- TM39 Rippon GD, leGras CAA, Hyne RV & Cusbert PJ 1992. *Toxic effects of cyanide on aquatic animals of the Alligator Rivers Region*. Technical memorandum 39, Supervising Scientist for the Alligator Rivers Region, AGPS, Canberra. (17pp)
  
- TM40 Devonport CC 1992. *A selected GIS bibliography*. Technical memorandum 40, Supervising Scientist for the Alligator Rivers Region, AGPS, Canberra. (91pp)
  
- TM 41 Roberts RG, Uren CJ & Murray AS 1993. *Thermoluminescence dating techniques at the Alligator Rivers Region Research Institute*. Technical memorandum 41, Supervising Scientist for the Alligator Rivers Region, AGPS, Canberra. (63pp)
  
- TM42 Rippon GD & Chapman JC 1993. *Laboratory procedures for assessing effects of chemicals on aquatic animals*. Technical memorandum 42, Supervising Scientist for the Alligator Rivers Region, AGPS, Canberra. (26pp)
  
- TM43 Dostine PL, Humphrey CL & Faith DP 1993. *Requirements for effective biological monitoring of freshwater ecosystems*. Technical memorandum 43, Supervising Scientist for the Alligator Rivers Region, AGPS, Canberra. (26pp)
  
- TM44 Devonport C & Waggitt PW 1994. *Geographic information systems and remote sensing in northern Australia: A compendium*. Technical memorandum 44, Supervising Scientist for the Alligator Rivers Region, AGPS, Canberra. (60pp)
  
- TM45 Akber RA and Pfitzner JL 1994. *Atmospheric concentrations of radon and radon daughters in Jabiru East*. Technical memorandum 45, Supervising Scientist for the Alligator Rivers Region, AGPS, Canberra. (23pp)
  
- TM46 Finlayson CM, Thompson K, von Oertzen I & Cowie ID 1994. *Vegetation communities of five Magela Creek billabongs, Alligator Rivers Region, Northern Territory*. Technical memorandum 46, Supervising Scientist for the Alligator Rivers Region, AGPS, Canberra. (32pp)
  
- TM47 Akber Riaz & Martin Paul (eds) 1994. *Techniques for the analysis of radionuclides in the environment and their application: Part 1*. Technical memorandum 47, Supervising Scientist for the Alligator Rivers Region, AGPS, Canberra. (64pp)
  
- TM48 Waggitt Peter 1994. *A review of worldwide practices for disposal of uranium mill tailings*. Technical memorandum 48, Supervising Scientist for the Alligator Rivers Region, AGPS, Canberra. (52pp)

## Other publications

Supervising Scientist for the Alligator Rivers Region 1991. *Proceedings of the 29th Congress of the Australian Society of Limnology*. Jabiru 1990, Supervising Scientist for the Alligator Rivers Region, AGPS, Canberra. (135pp)

Devonport C, Riley SJ & Ringrose SM (eds) 1992. *Proceedings of the GIS and Environmental Rehabilitation Workshop*. Darwin 4-5 September 1992, Supervising Scientist for the Alligator Rivers Region, AGPS, Canberra. (161pp)

Akber RA (ed) 1992. *Proceedings of the Workshop on Land Application of Effluent Water from Uranium Mines in the Alligator Rivers Region*. Jabiru 11-13 September 1990, Supervising Scientist for the Alligator Rivers Region, AGPS, Canberra. (366pp)

Riley SJ, Devonport C, Waggitt PW & Fitzpatrick B (eds) 1993. *NARGIS 93: Proceedings of the North Australian Remote Sensing and Geographic Information Systems Forum*. Darwin 9-11 August 1993, Supervising Scientist for the Alligator Rivers Region and the Australasian Urban and Regional Information Systems Association Inc [Monograph no 8], AGPS, Canberra. (301pp)

Supervising Scientist for the Alligator Rivers Region (in press). *Proceedings of the Workshop on Biological Monitoring of Freshwater Ecosystems in Tropical Northern Australia*. 21-24 September 1993, Supervising Scientist for the Alligator Rivers Region, AGPS, Canberra. (... pp)

Riley SJ, Waggitt PW & McQuade C (eds) 1993. *Proceedings of the Symposium on the Management and Rehabilitation of Waste Rock Dumps*. Darwin 7-8 October 1993, Supervising Scientist for the Alligator Rivers Region, AGPS, Canberra. (182pp)

Akber RA & Harris F (eds) 1994. *Radon and radon progeny measurements in Australia*. Symposium, Canberra 18 February 1994, Supervising Scientist for the Alligator Rivers Region, AGPS, Canberra.

SSARR (Supervising Scientist for the Alligator Rivers Region) 1992. *Supervising Scientist for the Alligator Rivers Region: Annual report 1993-94*. AGPS, Canberra.